

V. Potential Future Conditions of the Sonoran Desert

Potential future conditions for near-term (2025) development, long-term potential energy development, near-term terrestrial landscape and aquatic intactness, and potential mid-century (2060) climate change impacts were examined through the use of fuzzy logic modeling. Results for each analysis (i.e., land area in various classes) overlaid on the distribution of the core conservation elements—wildlife species, vegetation communities, and designated lands—assessed the proportion of each conservation element distribution in the various intactness or potential development classes. Lack of source data for future projections was common resulting in underestimates of what is likely to occur in the near-term future (2025) time frame.

Near-term development and intactness project from the present to 2025. Maximum potential (or long term) energy development has an indeterminate time frame. The potential energy development analysis considered all potential known traditional and renewable energy data sources; it is based on polygons representing energy zones rather than specific leases or applications. For this reason, maximum potential energy development, as discussed in Section 5.2 below, when overlaid on conservation elements' distributions may overestimate the impacts to species, habitats, and sites. Projecting into the future is a challenging endeavor and the results should be viewed critically as they possess many uncertainties and should not be relied upon for detailed site-level planning and management without additional data and analysis. Details on the relative quality of data sources for near term and potential development may be found in Appendix E. Tables listing data sources give the relative quality of each data set and a rating of overall model performance or certainty (based on best professional judgment). The results provide future scenarios for the ecoregion based on available projection data and show how the predicted changes may affect the various conservation elements of interest.

5.1 Projected Near-term Future (2025) Development

Projected near-term future (2025) development was built from the current development fuzzy logic model, which is comprised of four major development components—energy, agriculture, urban and roads, and recreational development (Figure 5-1). In reality, all of these factors are likely to change, but there were little predictive data available to use that provided meaningful projections into the future. The renewable energy development footprint included 2011 renewable energy project points and solar priority projects. (Note: a map of near-term renewable energy development locations relative to the distribution of the two desert tortoise species may be found in the Desert Tortoise Case Study Insert.) There were no data available for the near-term expansion of linear utilities. There were also no datasets for projected future for either intensive agriculture or grazing. Given climate change results and the overallocation of water resources, the future of agriculture is uncertain. Current recreation data were difficult to acquire and assemble; as a result, there were no changes made in recreation for the near-term. Future projections for urban development were based on model results from Theobald (2010), but there were no accompanying data on projected road building, which is a noteworthy deficiency as the effects of road impacts on many wildlife species and overall intactness is well known. Even with the lack of important topical data, some measurable changes were observed (Table 5-1). The Very High development class increased by 1.5% and both High and Moderately High classes gained approximately .5% over the near term future time period to 2025. The area covered by the four major development components expanded by over 887,000 acres region-wide during this time period. All of the results from the development model were incorporated into the near-term intactness models. The potential impact on conservation elements from near-term future development was examined by overlaying the near-term future (2025) intactness modeling results on conservation element distributions as described in Section 5.3 (and Appendices B and C).

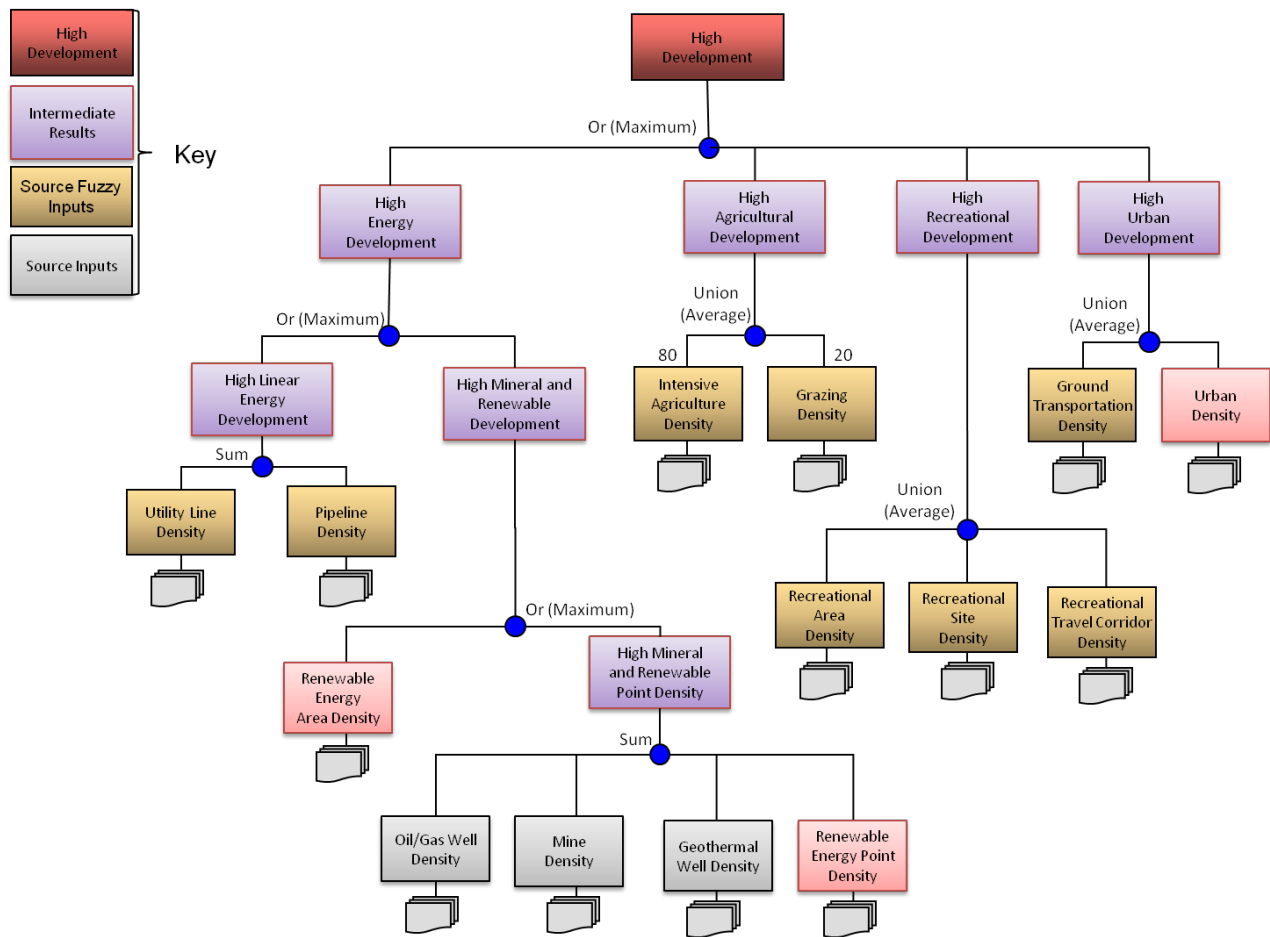


Figure 5-1. Fuzzy logic model for future near-term (2025) development for the Sonoran Desert ecoregion. Pink boxes depict the inclusion of additional data.

Table 5-1. Modeled change in land area (in 1000s of acres) for current to near-term future (2025) development for the Sonoran Desert ecoregion.

Category	Current	Percent	Near-term	Percent	Change
Very High	3,996	11.4%	4,531	12.98%	+1.5%
High	2,179	6.2%	2,328	6.67%	+0.4%
Moderately High	2,033	5.8%	2,236	6.40%	+0.6%
Moderately Low	5,652	16.2%	5,304	15.19%	-1.0%
Low	9,230	26.4%	8,868	25.40%	-1.0%
Very Low	11,825	33.9%	11,648	33.36%	-0.5%

5.2 Potential Energy Development

This section focuses on maximum potential energy development (mostly renewable energy) that could foreseeably occur beyond 2025. Maximum potential energy development was analyzed with a fuzzy logic model that included three major components—traditional oil and gas, wind energy, and solar energy (Figure 5-2). Potential for oil, gas, and geothermal development was created by simply buffering existing wells (not shown). Solar resource potential, defined as $>5.5 \text{ kW/m}^2$ in areas with $< 1\%$ slope, was obtained from the National Renewable Energy Laboratory (NREL, www.nrel.gov/rredc/, Figure 5-3) and added to solar priority projects, selected features from California BLM on verified and preliminary renewable energy rights-of-way, revised solar energy zones (SEZs), and Arizona Restoration Design Energy Project data (RDEP). Potential wind development was also comprised of NREL data and defined by wind power density classes 3 and above at 50 m high (Figure 5-4).

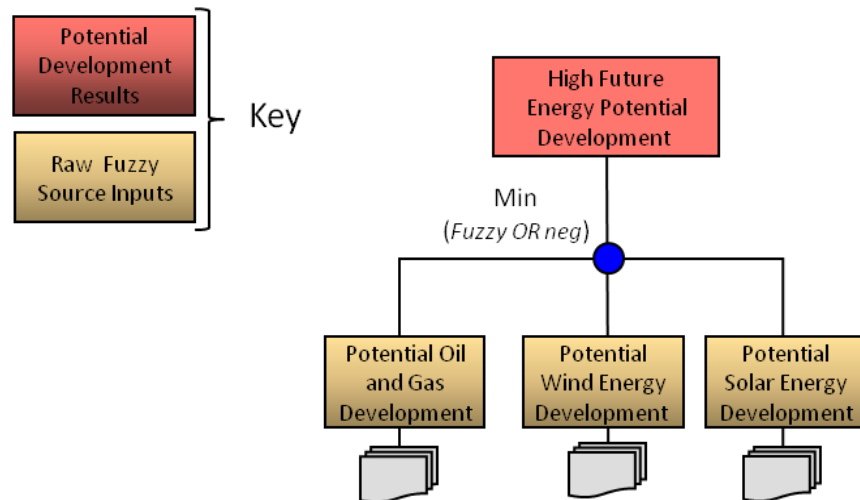


Figure 5-2. Fuzzy logic model diagram for maximum potential energy development in the Sonoran Desert ecoregion.

Summarized at 4km resolution, the final composite map for all three energy components showed about 32% of the area of the ecoregion subject to moderate or high potential energy production (Figure 5-5). Values from the fuzzy logic model were divided into three basic classes (High 1 to 0.33, Moderate 0.33 to -0.33, and Low -0.33 to -1) instead of the six classes that have been used in other fuzzy logic models (such as the intactness models and the model for near-term [2025] development); finer differentiation was not depicted or warranted as the subject data covered broad areas and were more speculative (that is, not based on actual plans for development). For the ecoregion, over 7 million acres (or about 21%) were classified as having High potential, about 3,900,000 acres (11%) Moderate potential, and the rest, almost 24,000,000 acres (68%) Low potential. These results, when overlaid with the distribution maps for all of the conservation elements, evaluated the potential impact for each element from potential energy development. As mentioned earlier, maximum potential development of energy resources may overestimate the impacts to species, habitats, and sites since full development is not likely to be realized. Designated lands were not included in this part of the analysis because most energy development is prohibited from these areas.

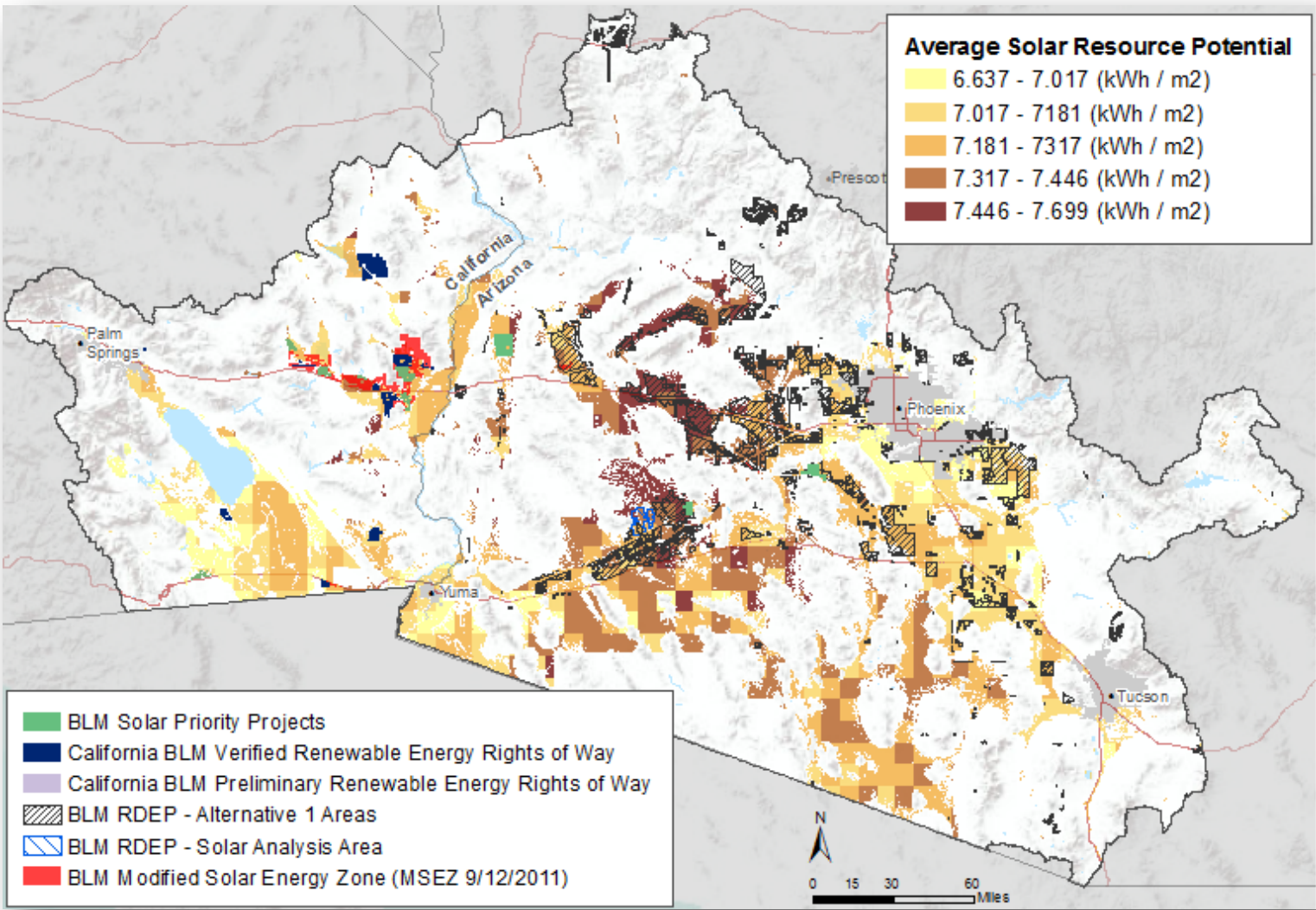


Figure 5-3. Solar energy source data for the maximum potential energy development model for the Sonoran Desert ecoregion including BLM solar priority projects (green), Arizona BLM RDEP areas (hatched), solar energy zones (SEZs in red), and NREL average solar resource potential polygons (yellow, orange polygons).

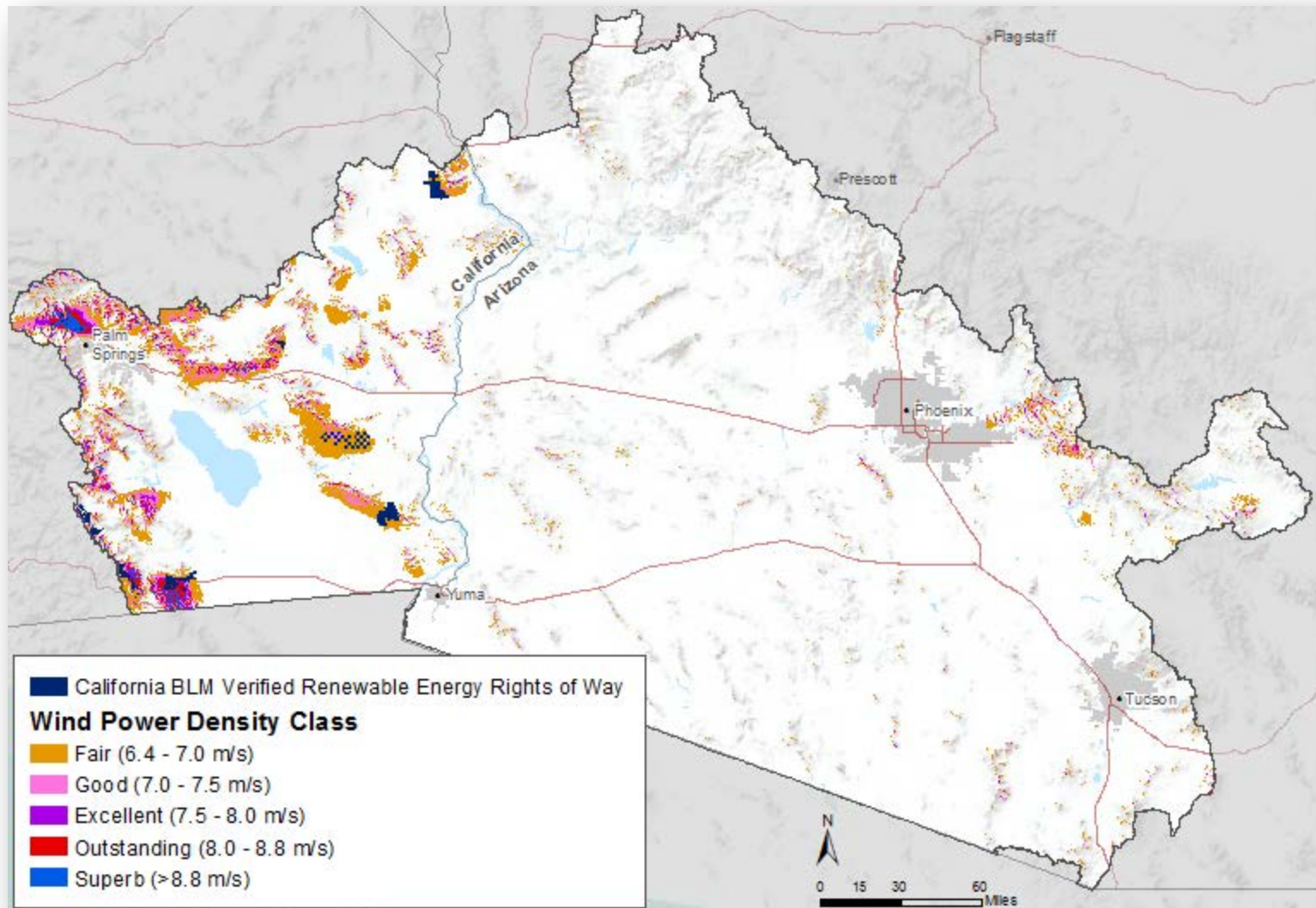


Figure 5-4. Wind energy source data (wind power density classes 3 and above at 50 m high) for the maximum potential energy development model for the Sonoran Desert ecoregion including California BLM renewable energy rights of way and five wind power density classes.

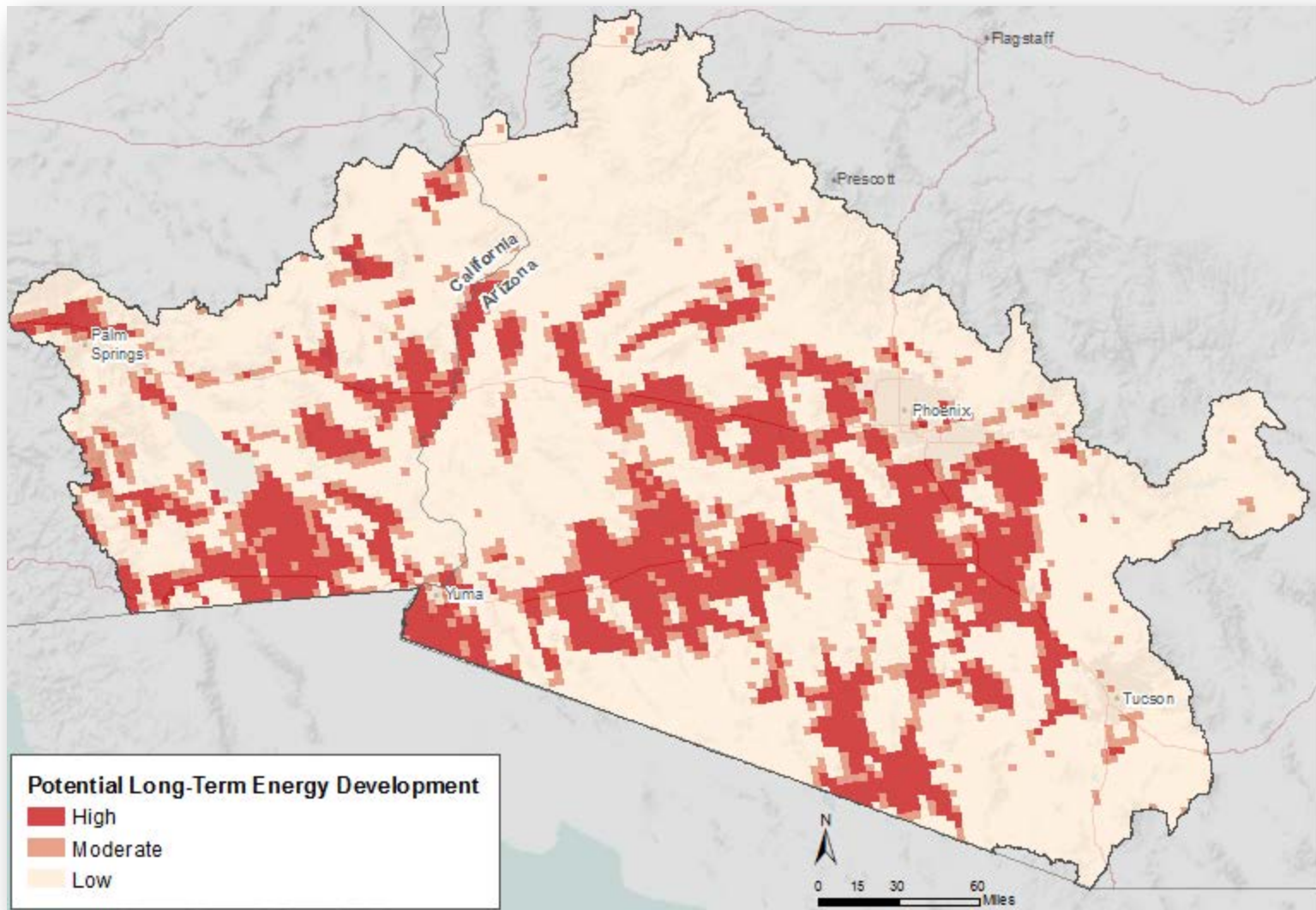
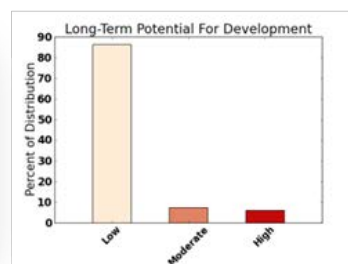


Figure 5-5. Map of maximum potential energy development for all three energy components (wind, solar energy, and oil and gas [not shown as source map]) in the Sonoran Desert ecoregion. Because of the more speculative nature of the data, values from the fuzzy logic model were divided into three basic classes (High 1 to 0.33, Moderate 0.33 to -0.33, and Low -0.33 to -1), rather than six classes as for the intactness models.

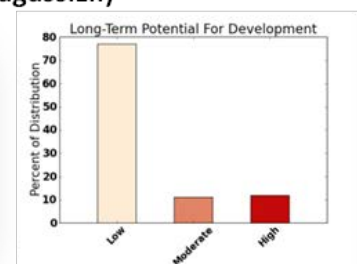
5.2.1 Impact of Potential Energy Development on Wildlife Species

Potential impact on species conservation elements from maximum potential (or long term) energy development varied greatly among species (Figure 5-6). Of the three mammal species examined, mule deer showed the greatest potential impact (with approximately 15% of its current distribution affected). Mountain lion was second with 8% and desert bighorn sheep followed with around 4% of its current distribution potentially under high impact from energy development. Of the two tortoise species, Mojave desert tortoise (*Gopherus agassizii*) was more highly affected than Sonoran desert tortoise (*Gopherus morafkai*) because of its occurrence in renewable energy zones. Although the lowland leopard frog was evaluated for near-term (2025) landscape intactness and status, it was not evaluated for maximum potential energy development because it was treated as an aquatic species.

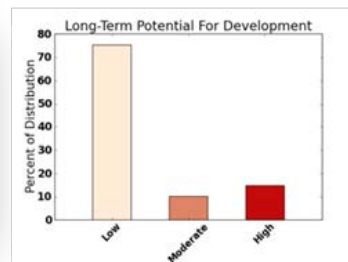
Mountain Lion



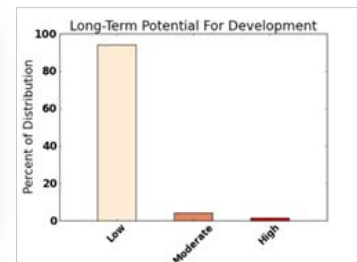
Desert Tortoise (agassizii)



Mule Deer



Desert Tortoise (morafkai)



Desert Bighorn Sheep

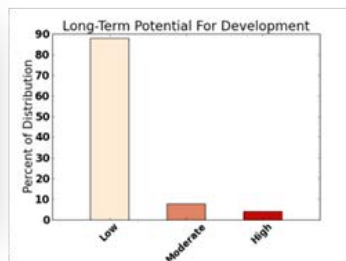
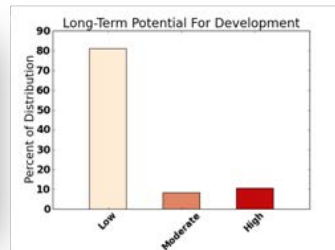


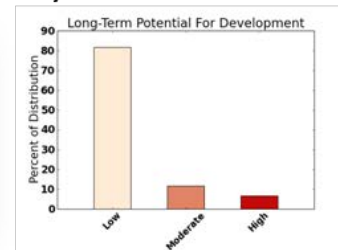
Figure 5-6. Impact from maximum potential (long term) energy development on the mammal and reptile conservation elements of the Sonoran Desert ecoregion. Values from the fuzzy logic model were divided into three basic classes (High 1 to 0.33, Moderate 0.33 to -0.33, and Low -0.33 to -1). For more information on the tortoise species, see the desert tortoise insert. For more details on mammal species, see Appendix C.

Between 70–80% of current bird species’ distributions were considered to be under low threat from energy development (Figure 5-7). Le Conte’s thrasher, a resident of creosote-bush flats, showed the highest level of threat with 18% and 12% of its current distribution under High and Moderate threat, respectively. Although the data over-represented Le Conte’s thrasher distribution, the bird is rare even in optimal habitats, and it requires large blocks of intact creosotebush habitat to persist. Thorough inventories for species like Le Conte’s thrasher or desert tortoise with large area needs should precede any planning in solar energy zones. All of the other birds had roughly 20% of their current distributions under potential threat from future development. Southwestern willow flycatcher distribution covers about 139,000 acres in the ecoregion (based on USFWS critical habitat data, [2005, 2011], <http://ecos.fws.gov/speciesProfile/profile>), which may or may not be occupied), and, according to the potential energy development model, the species could potentially lose 20,000 acres of this habitat, increasing the threat to its survival. Potential losses to riparian species from long-term energy development appear to be based on the potential development of NREL solar resource areas near the Colorado and Gila rivers.

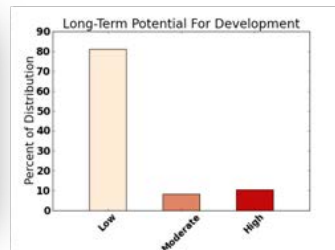
Golden Eagle



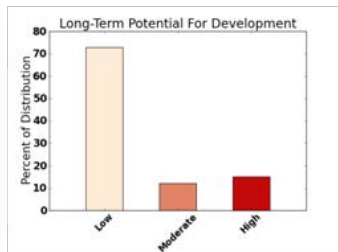
Southwest Willow Flycatcher



Lucy’s Warbler



LeConte’s Thrasher



Bell’s Vireo

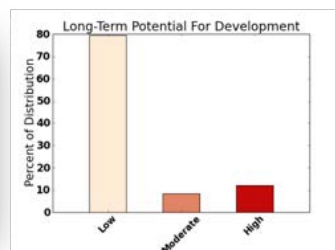


Figure 5-7. Impact from maximum potential (long-term) energy development on the bird species conservation elements of the Sonoran Desert ecoregion. Values from the fuzzy logic model were divided into three basic classes (High 1 to 0.33, Moderate 0.33 to -0.33, and Low -0.33 to -1). For background material on individual species, see Appendix C.

5.2.2 Potential Energy Development Impact on Vegetation Communities

Of the three vegetation communities examined, Sonoran-Mojave Creosotebush-White Bursage Desert Scrub showed the greatest potential impact with as much as 30% of its current distribution within the High class (Figure 5-8). Riparian vegetation also showed fairly high vulnerability with nearly 20% in the High category. The two classification systems for the two matrix vegetation communities, based on different interpretations of land cover imagery, showed the NatureServe version higher for the Sonoran-Mojave Creosotebush-White Bursage Desert Scrub and LANDFIRE existing vegetation data higher for the Sonoran Paloverde-Mixed Cacti Desert Scrub. As before with the riparian birds, direct impacts to riparian vegetation were mostly due to the overlap of NREL solar potential polygons with river networks, although upland development near riparian areas with associated roads, utility lines, and other infrastructure will also alter riparian habitat quality.

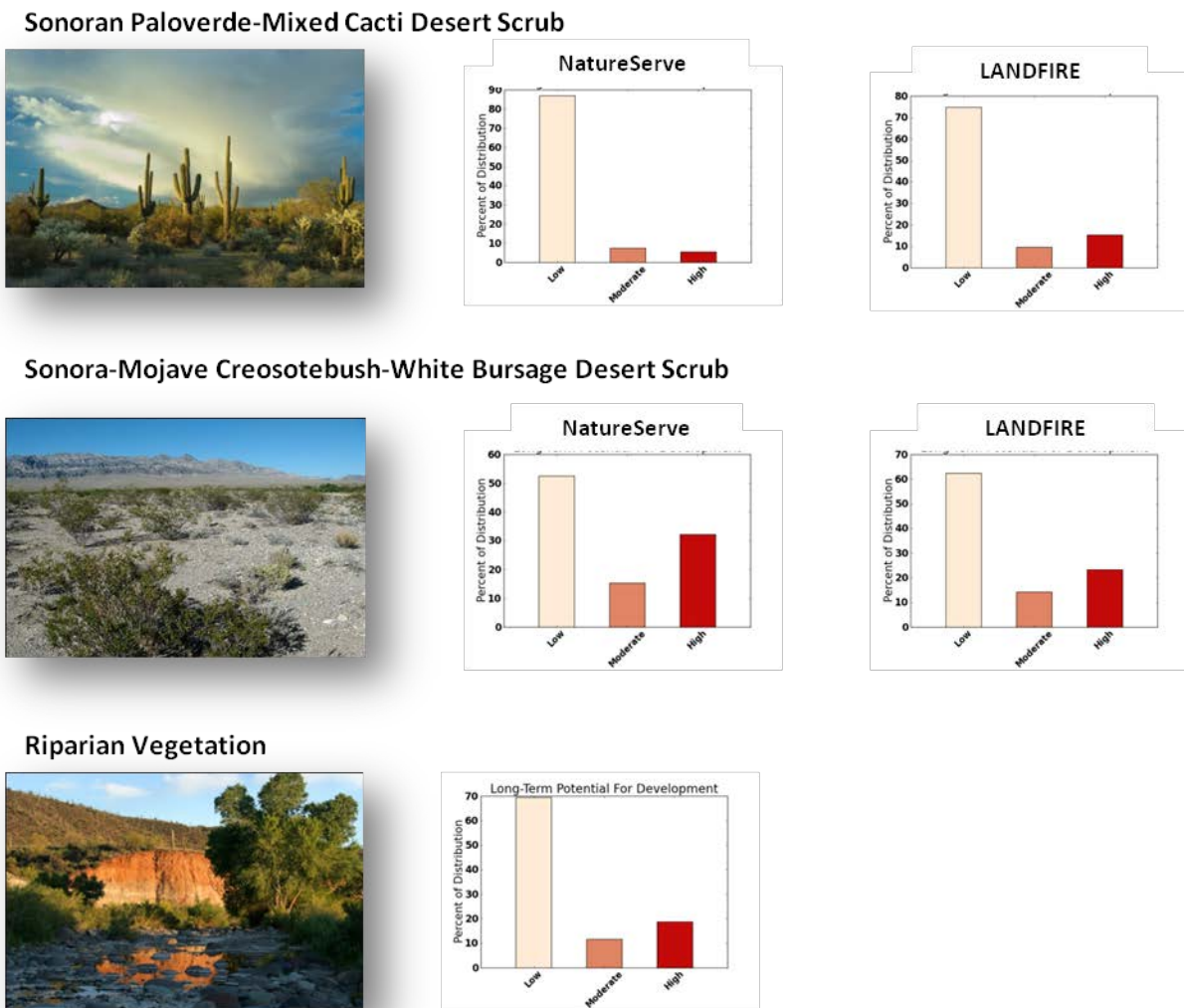


Figure 5-8. Histograms show impact from maximum potential (long-term) energy development on the vegetation communities of the Sonoran Desert ecoregion. Values from the fuzzy logic model were divided into three basic classes (High 1 to 0.33, Moderate 0.33 to -0.33, and Low -0.33 to -1). For more details on individual vegetation classes, see Appendix B.

5.3 Near-term Future (2025) Terrestrial Landscape Intactness

Near-term (2025) terrestrial landscape intactness (at both 4km and HUC5 reporting units) consisted of the same components and construction as the current intactness models with available projection datasets replacing those for current condition (Figure 5-9). Urban area, renewable energy, and invasive species projections (pink boxes in logic models) were updated for the near-term future terrestrial landscape intactness model. Projections on the spread of invasive species (Figure 5-10) were based on the potential expansion of Sahara mustard predicted by the MaxEnt model described earlier (in Chapter 3 and Section 4.3) using soil characteristics and future climate estimates from climate models presented in Section 5.4. The map (Figure 5-10) represents all invasive species, although Sahara mustard was the only species that could be projected into the future. The apparently limited expansion of Sahara mustard shown in the near-term future model results (red in Figure 5-10) may have occurred because the current distribution model may have over-represented the species' distribution, based as it was on general climate and soil characteristics.

FRAGSTATS was not rerun because there was not enough additional information on fragmentation and rerunning it would only have added additional uncertainty to the results. The near-term future intactness results were overlaid on the distribution data for each of the conservation elements to predict their change in status from the near-term change agents for which data were available.

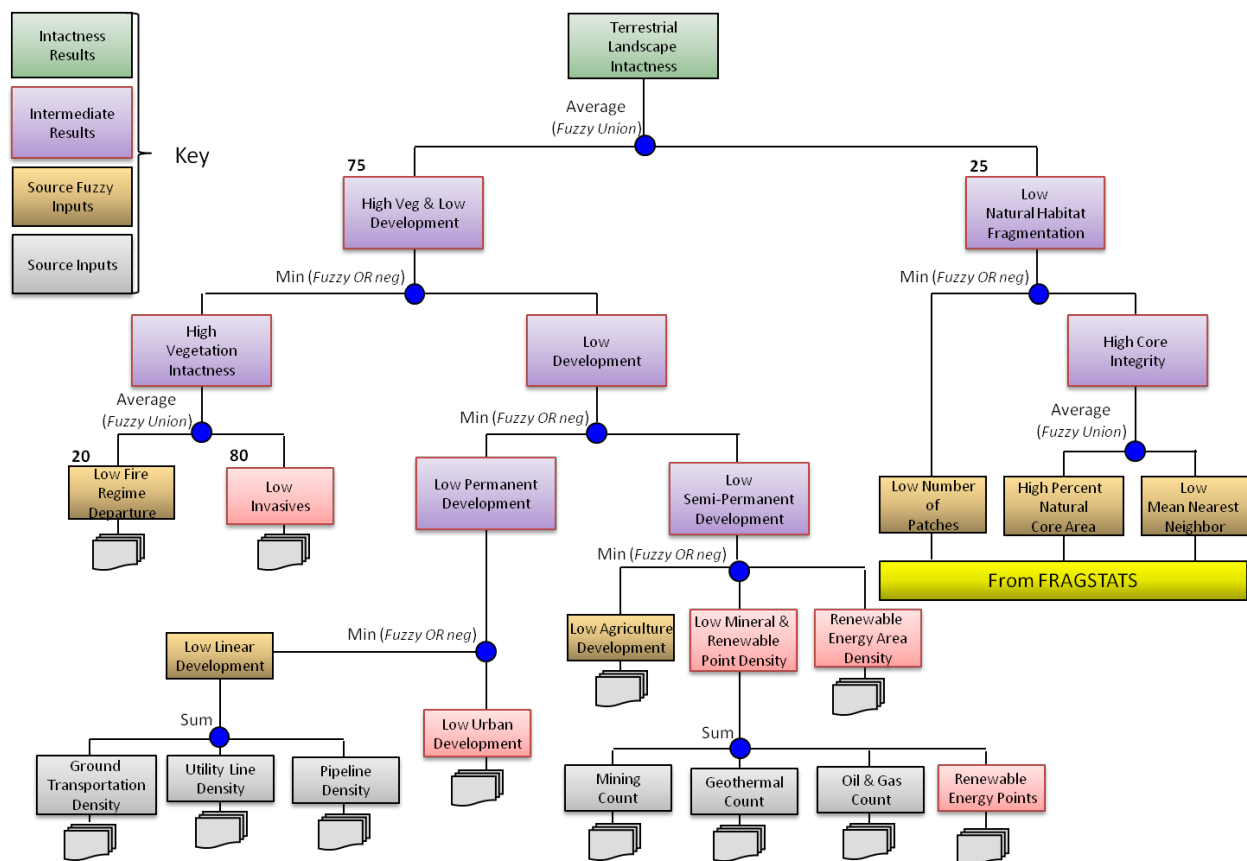


Figure 5-9. Near-term future (2025) terrestrial landscape intactness fuzzy logic model. Projection data inputs appear as pink boxes. Tables listing data sources and their relative quality and an overall confidence rating for the model may be found in Appendix E.

Overall, near-term future intactness in the ecoregion showed some declines with modest decreases in High and Moderately High intactness area countered by slight increases in the Low and Very Low classes (Figure 5-11, Table 5-2). Declines occurred in areas expected from the type of projected data input—near the Phoenix-Tucson urban corridor, the renewable energy zones, and along major interstate highways. The model could be improved with the addition of data on projected utility corridors, projected road density increases, and recreation. In Appendix E, tables list data sources represented in the logic model with their relative quality.

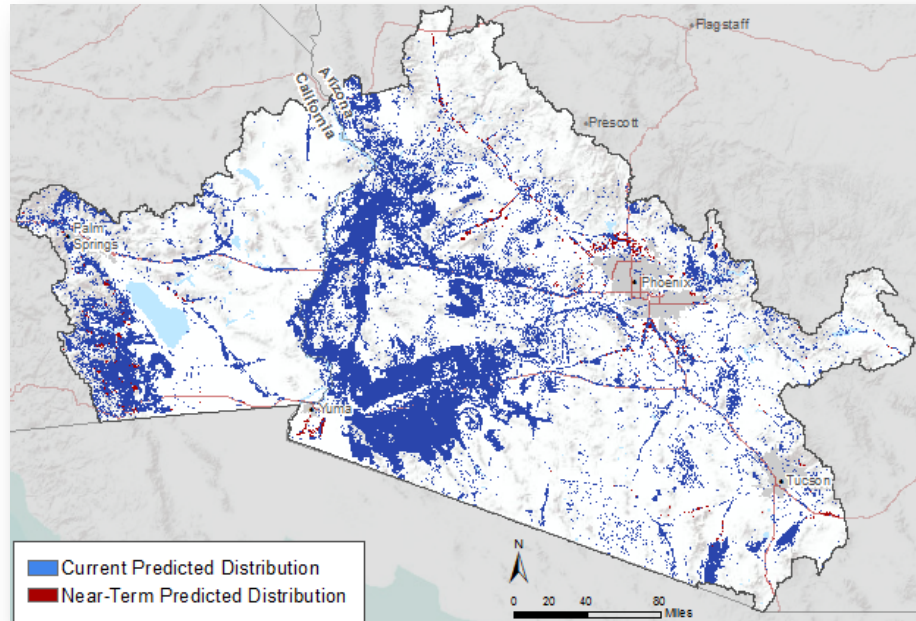


Figure 5-10. Current and near-term future (2025) predicted distribution of four invasive species selected as conservation elements. Expansion of invasive species (in red) is for modeled potential distribution of Sahara mustard only.

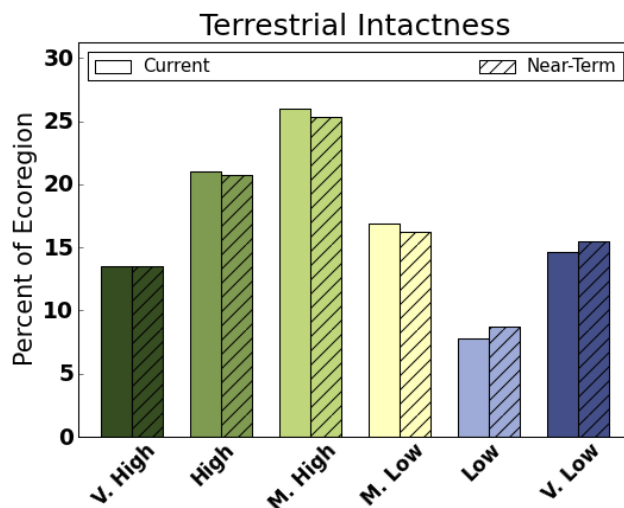


Figure 5-11. Histogram comparing current (solid color bars) and near-term future (hatched bars) terrestrial landscape intactness for the Sonoran Desert ecoregion showing small decreases in Very High and High intactness areas countered by slight increases in the Low and Very Low classes.

Table 5-2. Change in current to near-term future (2025) terrestrial landscape intactness (in 1000s of acres) for the Sonoran Desert ecoregion.

Category	Current	Percent	Near-term	Percent	Change
Very High	4,725	13.5%	4,713	13.5%	-0.03%
High	7,333	21.0%	7,234	20.7%	-0.28%
Moderately High	9,095	26.1%	8,840	25.3%	-0.73%
Moderately Low	5,910	16.9%	5,679	16.3%	-0.66%
Low	2,731	7.8%	3,036	8.7%	+0.87%
Very Low	5,121	14.7%	5,412	15.5%	+0.83%

5.3.1 Near-Term Future (2025) Status for Terrestrial Wildlife Species

Current and near-term status for each conservation element was based on the terrestrial landscape intactness models for the two time periods using the 4 km X 4 km resolution grid. Results pertain to the distribution area of each element at the finest scale (1:24,000) or resolution (30m pixels) available overlaid with the intactness results.

All mammals showed some declines (Figure 5-12) with mule deer and mountain lion distributions showing somewhat greater impact than desert bighorn sheep.

Mule deer and mountain lion showed similar response to near-term change (Figure 5-12 and Figure 5-13A) when using the same thresholds for the model variables. When the road threshold was applied to the model for mountain lion described in Chapter 4 (0.60 km/km², Van Dyke et al. 1986), the declines in mountain lion viability were more dramatic (Figure 5-13B). The declines are evident, not from the addition of potential roads data (projections on roads were not available), but because road densities representing true (or +1 in fuzzy logic) are constrained in the model to a level that does not negatively affect mountain lion (according to Van Dyke et al. [1986]). This is one example of the flexibility of a modeling process that allows quantifiable threshold information to be inserted as it becomes available.

All of the bird species showed declines in habitat quality in near-term future status, particularly the riparian species Bell’s vireo and southwestern willow flycatcher that are already in decline (Figure 5-14). Bell’s vireo is represented in the Sonoran REA as two distinct subspecies, Arizona Bell’s vireo (*Vireo bellii arizonae*) and least Bell’s vireo (*Vireo belli pusillus*). Arizona Bell’s vireo is state-listed as endangered in California (sensitive in Arizona), and least Bell’s vireo is both state and federally listed as endangered in California. Southwestern willow flycatcher is federally listed as endangered. Lucy’s warbler, also a sensitive riparian species at the northern extent of its range, does not fare as badly—possibly because of its greater adaptability to exploit alternative nesting habitats and food resources (see Appendix C). The fate of Le Conte’s thrasher parallels that of its habitat, creosotebush-white bursage, which continues to be converted and fragmented by urban and rural residential development and renewable energy development. Le Conte’s thrasher requires large contiguous patches of habitat and it will abandon blocks of creosotebush habitat undergoing fragmentation.

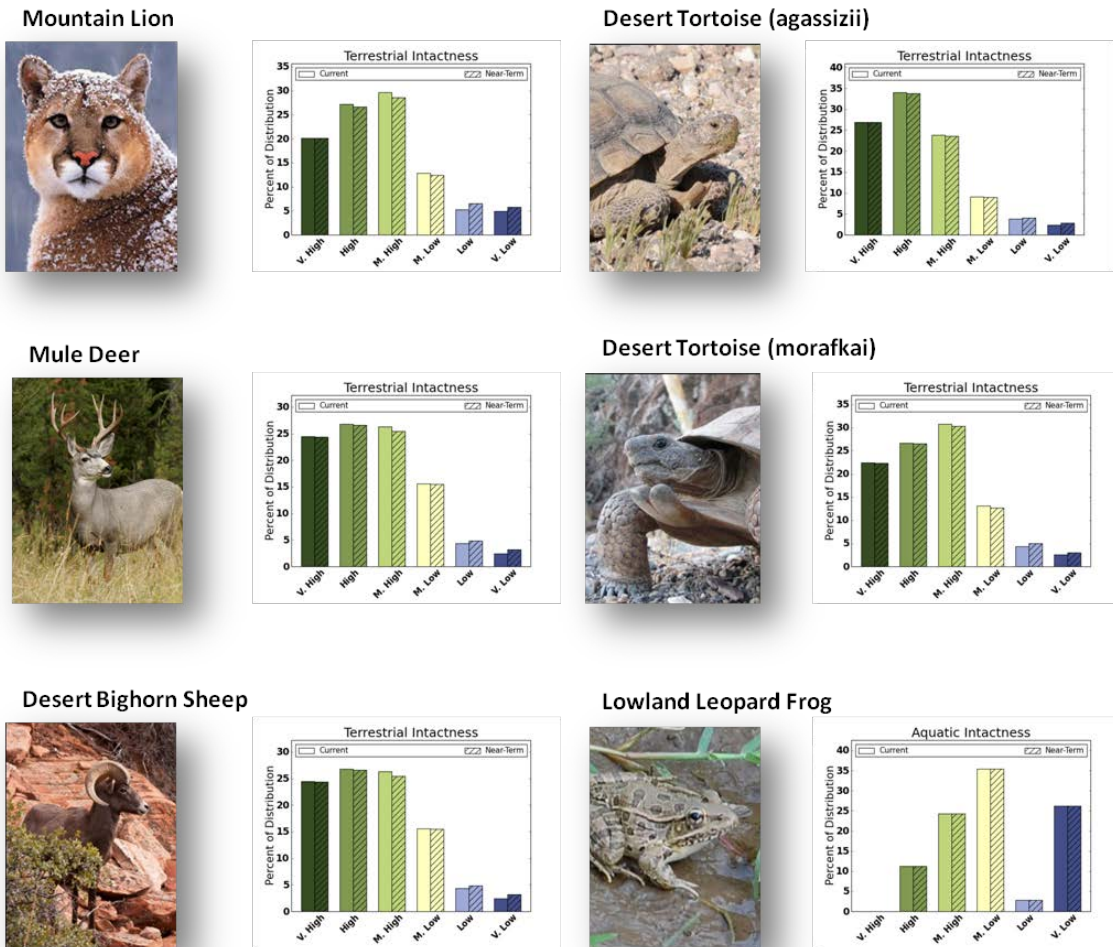


Figure 5-12. Comparison between current (solid) and near-term (crosshatched) future status for wildlife species conservation elements based on comparison of current distribution with current (solid) and near-term future (hatched) terrestrial landscape intactness.

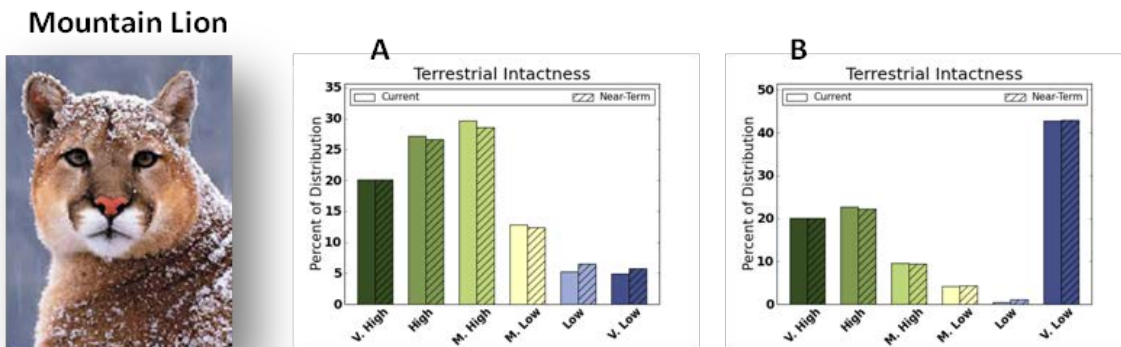


Figure 5-13. Comparison of current and near-term future status for mountain lion based on terrestrial landscape intactness for the (A) unconstrained model and (B) the constrained version imposing a road density threshold of 0.6 km/km² (Van Dyke et al. 1986).

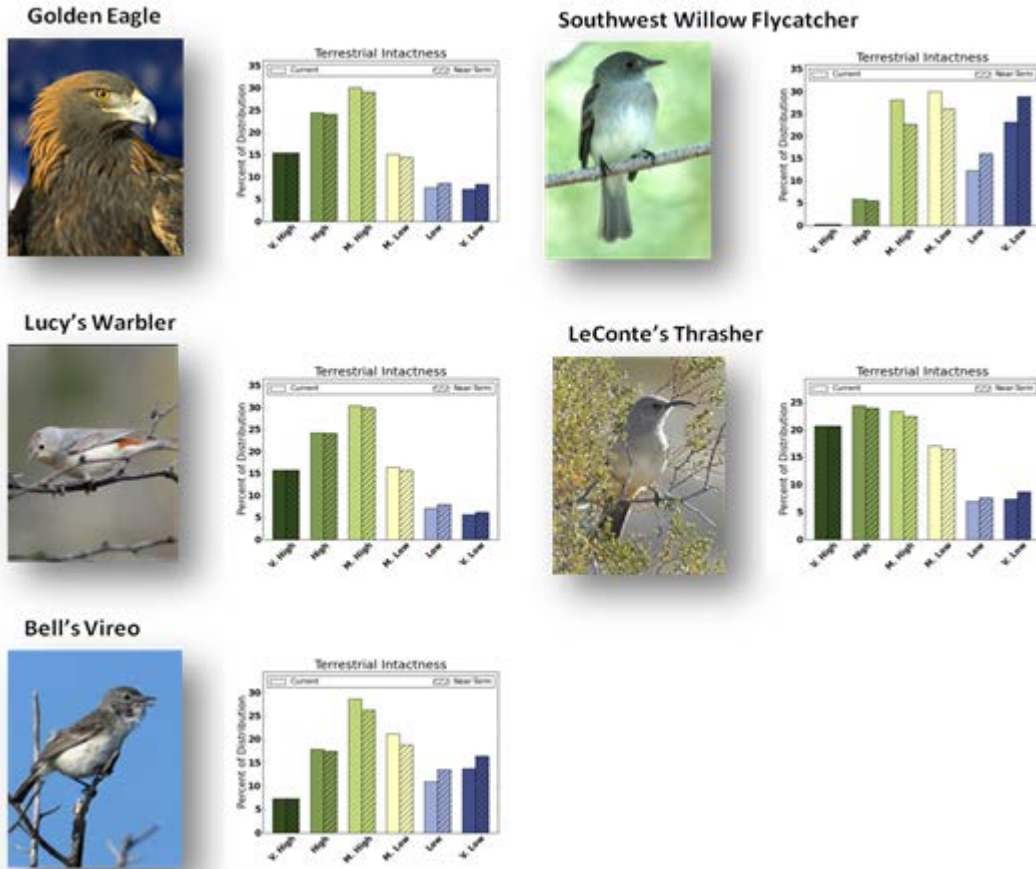
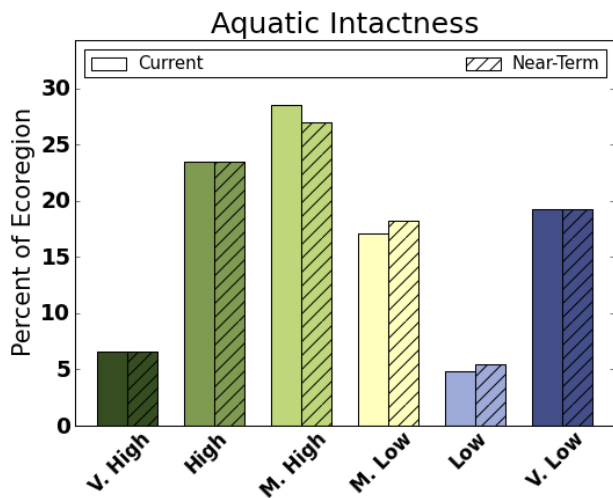


Figure 5-14. Comparison between current (solid) and near-term (crosshatched) future status for birds based on comparison of current distributions with current and near-term future terrestrial intactness.

5.3.2 Near-term Aquatic Intactness for Species Conservation Elements



The only change made in the aquatic intactness model was the addition of new urban areas for the 2025 time frame. No other data were available to populate the model whether it was planned dams and diversion changes, road construction, or chemical discharge and pesticide application changes. All of these elements affect aquatic systems, but there was no mechanism to predict them into the future (Figure 5-15).

Figure 5-15. Histogram shows comparison between current (solid bars) and near-term (crosshatched bars) aquatic intactness.

5.3.3 Near-term Future (2025) Status for Designated Lands

Results for near-term future intactness showed small percentage changes in the status of the existing designated protected lands in the Sonoran Desert ecoregion (Figure 5-16). Most of these changes are from the projected increase in invasive species, although some designated sites are already located near developed areas, some of which are expected to expand over time, further degrading lands around these sites. Information on the predicted near-term change in status for the remaining conservation elements (e.g., biodiversity sites, herd management areas) can be found in Appendix A.

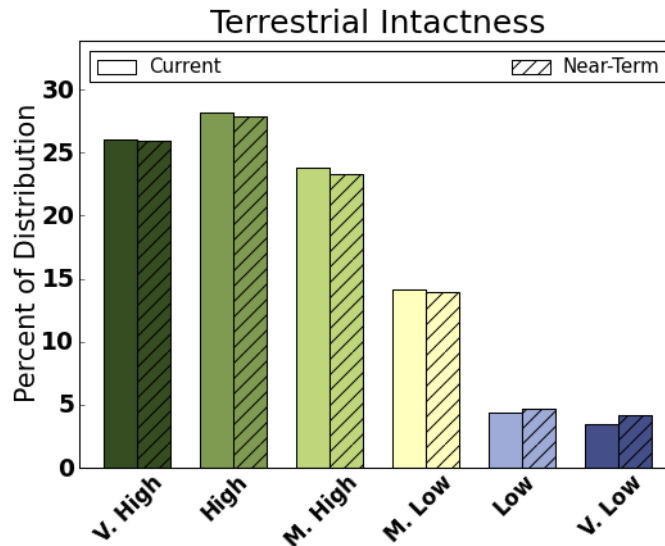
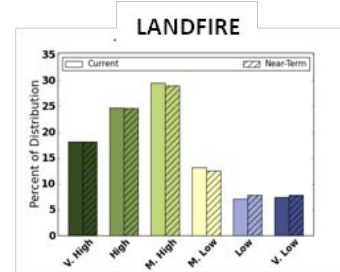
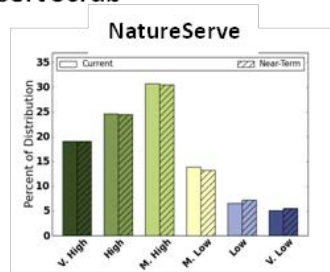


Figure 5-16. Current and near-term future (2025) status of designated lands in the Sonoran Desert ecoregion.

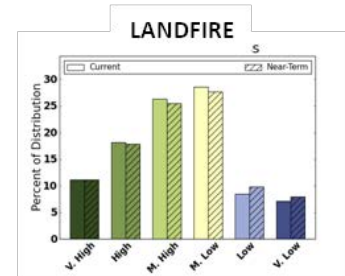
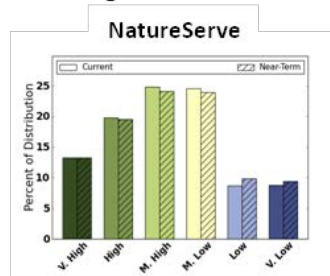
5.3.4 Near-term Future (2025) Status for Vegetation Communities

Near-term terrestrial intactness results showed habitat quality declines reflected as decreases in status for the matrix vegetation communities with the greatest declines observed for Sonoran-Mojave Creosotebush-White Bursage Desert Scrub (Figure 5-17), the vegetation community that is the focus of renewable energy development. Very little change is apparent in the Very High intactness categories for any of the vegetation communities. Overall ecoregion change in the Very High category was just -0.03%. This can be attributed to the fact that, based on the projected data used in the near-term logic model, most of the changes occurred in areas already affected or at the edges of expanding affected areas—in the Phoenix-Tucson corridor and along major highways. One might also assume that a high proportion of the remaining highly-intact areas are already well-protected (see also Figure 5-16). Riparian vegetation status showed some losses of intactness from the moderate categories to Low and Very Low intactness classes. Data were lacking in the model for a number of other potential stressors to riparian zones that are not expressed spatially (such as flow regime change or groundwater withdrawal) or that are evident only at a higher resolution (such as local clearing or riparian fire).

Sonoran Paloverde-Mixed Cacti Desert Scrub



Sonora-Mojave Creosotebush-White Bursage Desert Scrub



Riparian Vegetation

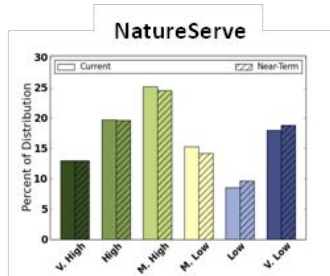


Figure 5-17. Histograms show the comparison between current (solid) and near-term (crosshatched) future status for vegetation communities for both the NatureServe and LANDFIRE landcover classifications for the Sonoran Desert ecoregion.

5.3.5 Application of Results for Near-Term Future Planning

As might be expected with any effort of this size and scope, the assessment raises as many questions as it answers. The REA provides a collection of data that can be queried and tested in innumerable ways. All that is required of the user is an understanding of the relatively coarse resolution of the mapped results and an ability to translate the results between scales, from regional to local. An understanding of the constraints and limitations of data at this scale is also necessary when considering current information as well as the near-term and long-term projections data. As has been noted, there was a general lack of data to populate the future development and intactness models. However, the value in having the logic model is that it provides a clear outline of the elements that must be acquired and inserted to improve the model results.

Several riparian species were selected as core conservation elements for the Sonoran Desert REA because of their importance and sensitivity. However, as discussed earlier, although the HUC and 4 km reporting units are appropriate for regional scale assessment, they are rather coarse for analysis of linear riparian features. On the other hand, riparian habitats are affected by upland disturbances and 4 km grid cells crossing riparian zones indicate nearby terrestrial changes as well as their effects on riparian areas.

An example of the projected future results for a riparian species will highlight the possibilities and problems involved in working with REA data. The results for southwestern willow flycatcher in Section 5.3.1, Near-term Status for Wildlife Species, indicate continued declines in status and potential habitat quality for a species already endangered (Figure 5-18). As presented in Chapter 4, status was determined by an overlay of the terrestrial intactness results with the species' distribution.

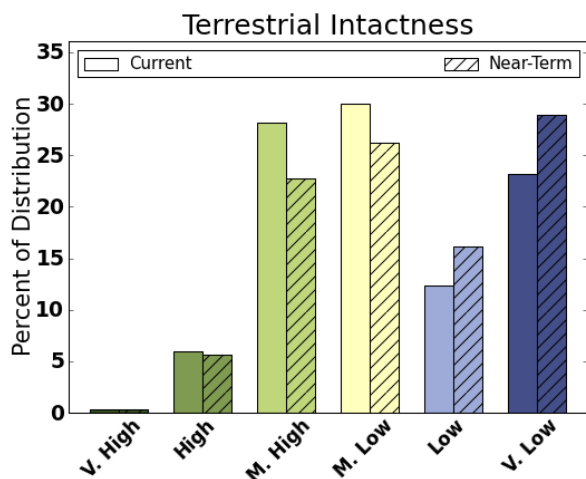


Figure 5-18. Histogram shows the changes in status between current (solid) and near-term future (2025, crosshatched) for southwestern willow flycatcher based on an overlay of current distribution with current and near-term future terrestrial intactness.

12–13% of the species' distribution changed from the High, Moderately High, and Moderately Low categories to Low and Very Low. These changes are large enough to be visible when comparing the current and near-term terrestrial intactness status results for the species in a map detail of the Colorado River from Lake Havasu to Parker Valley in the south (Figure 5-19); the red star is the location of Parker Dam near the confluence of the Bill Williams River, which also contains southwestern flycatcher critical habitat. Portions of grid cells within the bird's distribution change from Moderately High and Moderately Low to Low and Very Low in the two larger polygons in the upper and lower left quadrants of Figure 5-19A and B. One thing that becomes apparent when examining the data that produced these results is that the USFWS critical habitat polygons for southwestern willow flycatcher overlap the watery expanse of Lake Havasu, meaning that part of the 139,000 acres of the species' habitat is over-represented (see caption Figure 5-19). The next question is: What components of the near-term

future (2025) intactness model changed to create the change in future status for the species? The elements that changed in the logic model for near-term terrestrial intactness were renewable energy, invasive species, and urban development (pink boxes in Figure 5-8). The maps for near-term renewable energy development and the near-term spread of invasives (not shown) do not indicate any changes in this area near the Colorado River. The near-term (2025) changes come from modeled urban growth (Theobald 2010, Figure 5-20A).

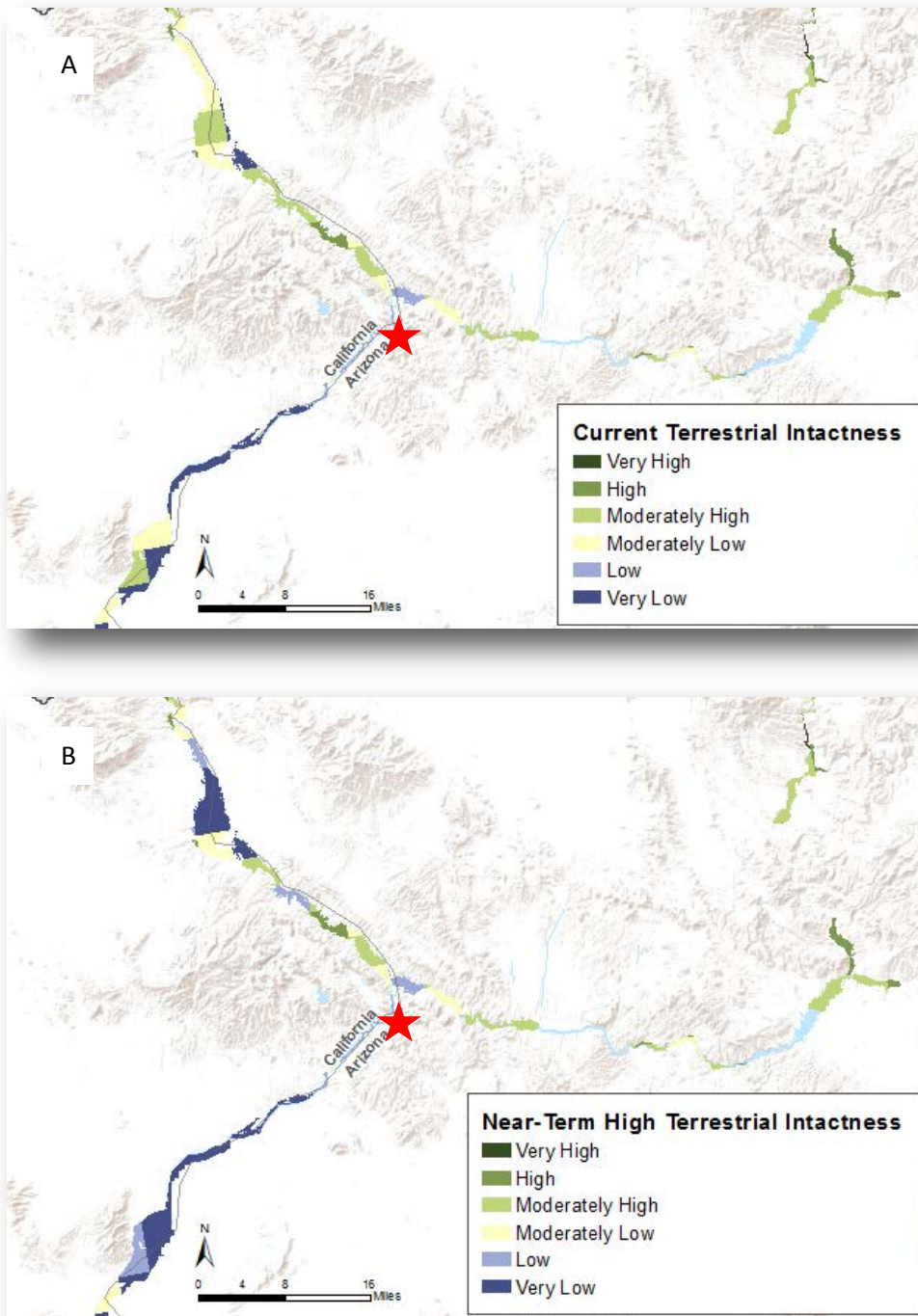


Figure 5-19. Maps comparing the (A) current and (B) near-term future (2025) terrestrial intactness-status results for the southwestern willow flycatcher in a map detail of the Colorado River from Lake Havasu to Parker Valley in the south. The red star is the location of Parker Dam near the confluence of the Bill Williams River, which also contains a significant amount of southwestern flycatcher critical riparian habitat. Changes in terrestrial intactness have occurred in the two larger polygons in the upper left and lower left quadrants of map 5-19B. USFWS critical habitat polygons for southwestern willow flycatcher overlap the watery expanse of Lake Havasu, meaning that a portion (19,300 acres) of the 139,000 acres of the species' habitat is over-represented. Users of the data may choose to use the NatureServe riparian data or remotely-sensed data for a higher-resolution comparison of riparian vegetation in areas of interest.

The modeled changes from urban growth projected for the lower left polygon on the maps (Figure 5-19A and B, Figure 5-20A) do not seem likely in the near term future as the location is an agricultural valley on the Colorado River Indian Reservation. On the other hand, the change in the polygon in the upper left quadrant, from Moderately High to Very Low intactness (Figure 5-19B) is more likely since it reflects projected changes in urban growth in grid cells in the vicinity of Lake Havasu City, Arizona and Havasu Lake, California (Figure 5-20A).

Although it is more speculative, projecting the status of the southwestern willow flycatcher further into the future (such as for maximum long-term energy development and climate change) may be linked in the same way to elements composing the models. As discussed in Section 5.2.1 (Impact of Potential Energy Development on Wildlife Species), according to the model for maximum potential energy development, southwestern willow flycatcher could lose as much as 20,000 acres of critical habitat (which may or may not be occupied) to long-term energy development. Based on the High and Moderate potential shown in the polygon in the lower left quadrant of the maximum potential energy development map (Figure 5-20B), potential losses to southwestern willow flycatcher along this section of the Colorado River appear to be based on the potential development of NREL solar resource areas (Figure 5-3); in this particular polygon, the areas of high potential for development lie on the east side of the Colorado River in agricultural land. It is possible to imagine that it may become profitable (more profitable than farming in the desert) for landowners to lease their property to solar energy firms just as they do now for wind turbines. This same polygon is in the Very High exposure category for long term potential for climate change (2060, not shown).

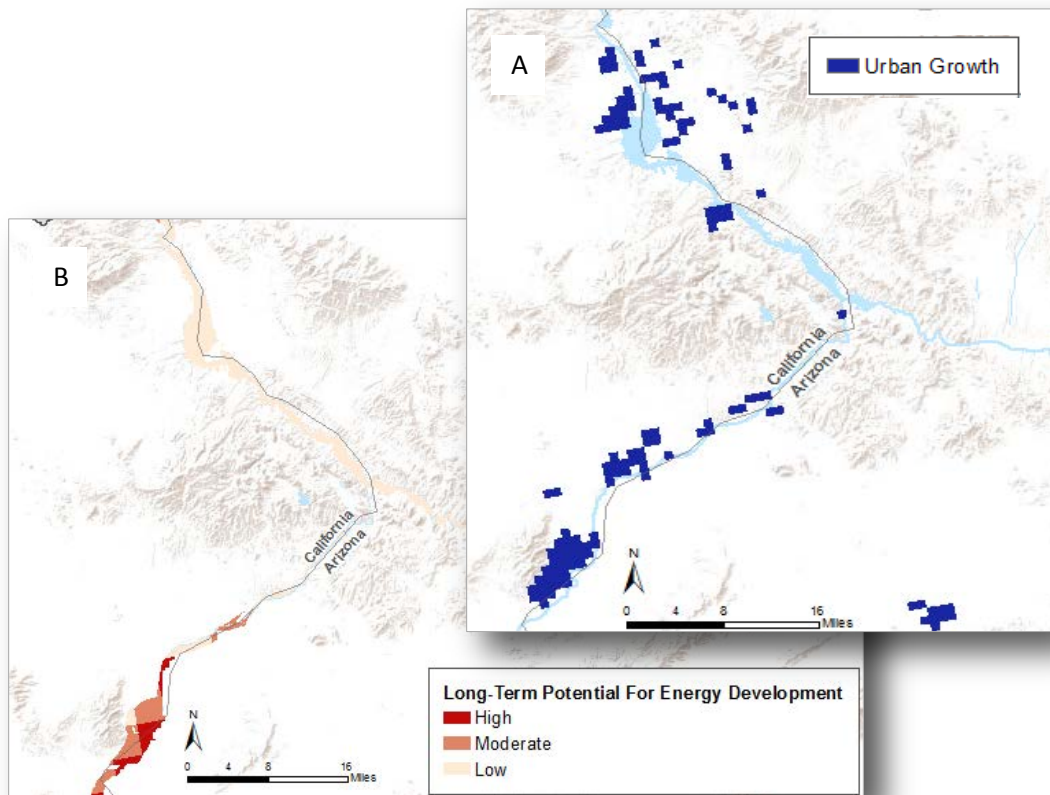


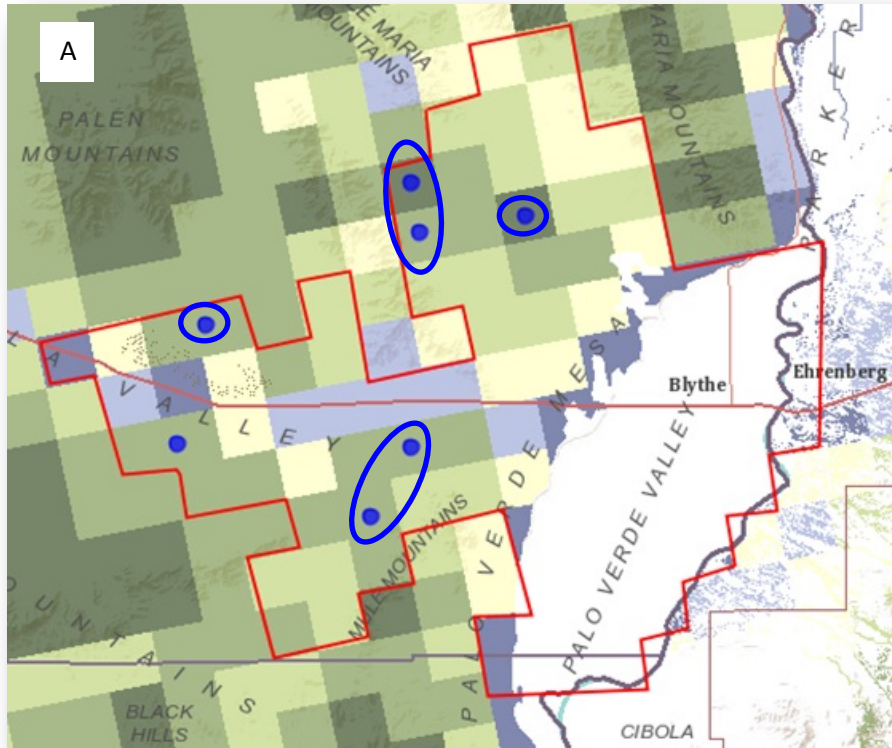
Figure 5-20. Map (A) Source data for modeled near-term future (2025) urban growth (Theobald 2010) showing projected growth pixels in the upper left (near Lake Havasu City) and lower left (Parker Valley). Map (B) Polygon at lower left shows high and moderate potential for change to southwestern willow flycatcher status from long term energy development based on overlap of NREL solar resource potential polygons.

This example shows the utility of examining the data in detail and becoming familiar with the strengths and weaknesses of the models and the underlying data sources. (Relative data quality and confidence in particular model results may be found in Appendix E.) Another important point related to the step-down process is that the models may not translate directly to on-the-ground realities or interpretations of species response. The different classes of intactness suggest corresponding levels of species status or condition, but the classes created for fuzzy logic model results do not have inherent ecological significance. The six intactness categories were selected to be easily understood and symmetrical around 0, so that degrees of “falseness” ranged from 0 to -1 and “trueness” from 0 to +1 (as explained in Section 3.2.3 Logic Models). While future users are free to change these categories, it may be simpler to retain the six intactness classes; the classes will gain ecological significance and meaning as they are calibrated with finer scale data and groundtruthing. With the top-down application of REA results, each user will create a personal crosswalk of meaning among the classes at various scales, both regional and local.

Another timely application of the near-term future results is in the planning, siting, and mitigation of renewable energy projects; renewable energy was an element of the logic model for which there were adequate predictive data in the form of solar and wind potential areas. An example of applying REA data and results to renewable energy planning is presented below for a portion of an NREL polygon and a Solar Energy Zone (SEZ), Riverside East, near Blythe, California. Riverside East contains nearly 148,000 developable acres; several applications had been authorized on 57,000 acres of this SEZ by the end of 2011. On the data portal, REA results for the matrix vegetation communities may be compared with mapped status and distribution for REA species of interest (represented here in Figures 21A and B and Figures 22 A and B) and the overlap noted for various status classes of habitats and species. For example, Figures 21A and B, depicting the SEZ and NREL areas outlined in red, compare the distribution of Le Conte’s thrasher (Figure 21A) with one of its major habitats, creosotebush-white bursage (Figure 21B). Two areas of interest (in Very High and High intactness classes) are the three topmost circled dots north of Interstate 10—near a xeroriparian corridor, McCoy Wash—and the two dots on the northwest slopes of the Mule Mountains south of the interstate. (Note: the white area on the vegetation map near the third dot in the north is a playa likely to have some saltbush vegetation, which also supports Le Conte’s thrasher). The fact that the distribution of Le Conte’s thrasher is likely highly over-represented does not invalidate this analysis. Any of the REA species data may be over-, under-, or mis-represented; the species data are composed of generalized range maps, (largely un-validated) SW ReGAP models, or mapped expert judgment information based on field experience. REA data will have to be validated as it is used. Also, potential habitat may or may not be occupied, but unfragmented blocks of habitat (and any amount of xeroriparian habitat) have future value whether presently occupied or not, particularly for species with large area needs such as Le Conte’s thrasher and desert tortoise. In addition, it is standard practice to survey potential development areas for species of concern, meaning that land managers are not likely to rely on generalized mapped data without field surveys.

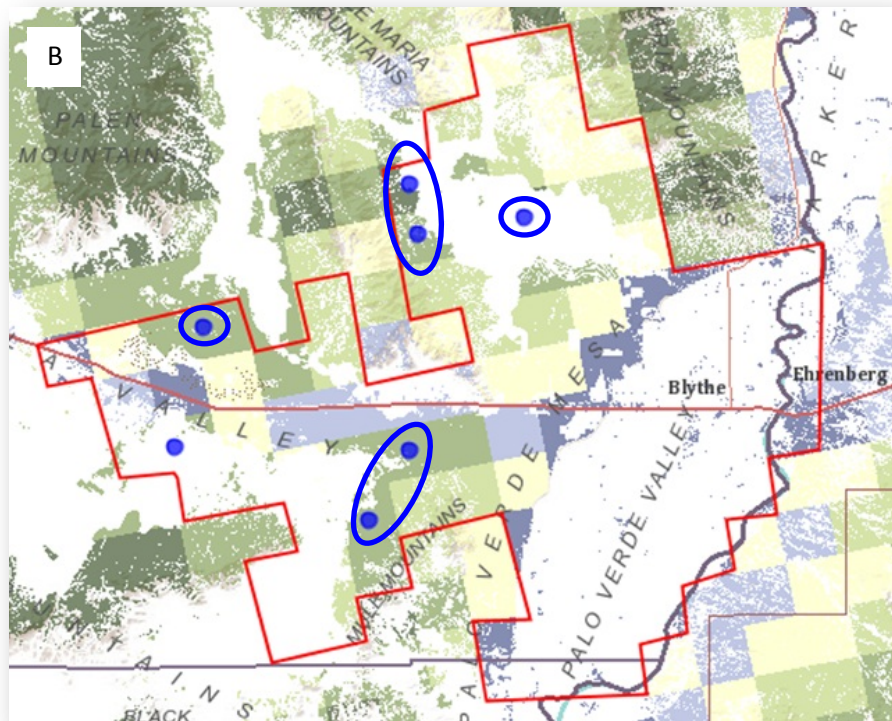
Continuing the renewable energy analysis with desert tortoise potential habitat (Figure 22A), any of the dots pictured inside or outside of mapped potential habitat appear to be in areas that may support desert tortoise (Chuckwalla Valley). Again, comparison of REA results with finer scale data is necessary. There is congruence of Very High and High modeled tortoise habitat with the previously-noted areas of interest for Le Conte’s thrasher near McCoy Wash and the northwest slopes of the Mule Mountains. For desert bighorn sheep (that appear to be absent from the entire SEZ area, Figure 22B), the obvious question to ask is why are there no bighorn sheep in the Big Maria and Little Maria Mountains? Are the Marias candidates for desert bighorn relocation? Could this area serve as a corridor for bighorn sheep movement from the south and southeast or is the interstate highway an impossible barrier to mitigate?

The test of the REA model results will be in their ultimate utility; the classes will gain ecological significance and meaning as they are applied and tied to local information. Higher resolution data and analyses may modify the results locally, but REA results will remain valid at the regional scale at which they were produced.



4KM Results: Current Status of Le Conte's Thrasher

- Very High
- High
- Moderately High
- Moderately Low
- Low
- Very Low



Current Status of Sonoran-Mojave Creosotebush-White Bursage Desert Scrub (NatureServe Landcover)

- Very High
- High
- Moderately High
- Moderately Low
- Low
- Very Low

Figure 5-21. Maps depict a Solar Energy Zone (SEZ) and NREL polygon outlined in red and compare (A) distribution and status of Le Conte's thrasher with (B) distribution and status of one of the thrasher's major habitats, creosotebush-white bursage, with circled common areas of interest (dots) in royal blue.

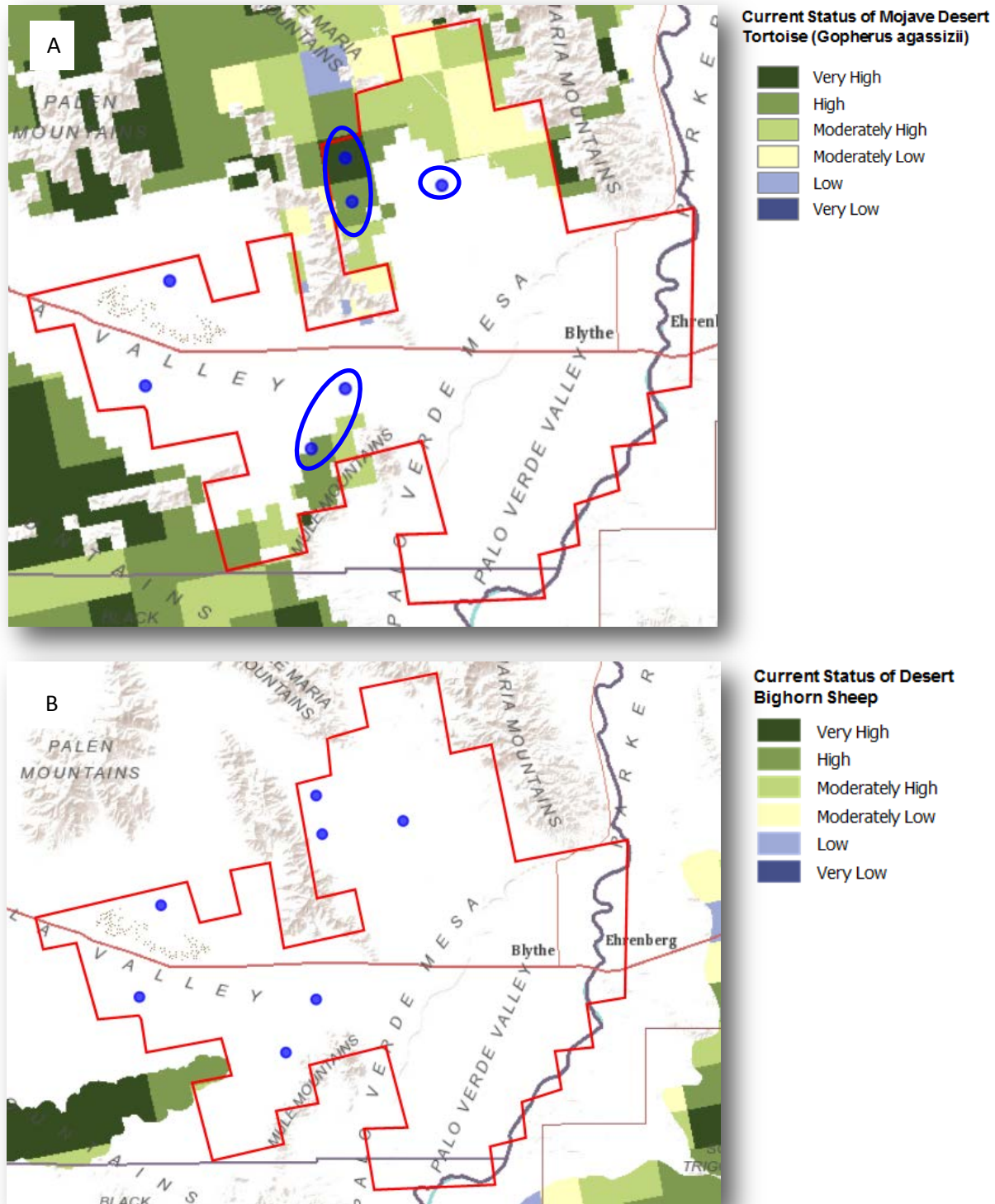


Figure 5-22. Maps compare (A) the distribution and status of the Mojave desert tortoise (*Gopherus agassizii*) with that of (B) desert bighorn sheep in a Solar Energy Zone (SEZ) near Blythe, California (boundary in red). Areas of interest and congruence with other REA species and habitats in Very High and High intactness classes are depicted as circled dots in royal blue.

5.4 Climate Change

Climate Change Management Questions

1. Where/how will the distribution of dominant native plants be vulnerable to or have potential to change from climate change in 2060?
2. Where are areas of potential species conservation element distribution change between 2010 and 2060?
3. Where are aquatic/riparian areas with potential to change from climate change?
4. Where are areas of potential surface water flow change?

Climate change results for the Sonoran Desert ecoregion are extensive and complex. This chapter focuses on answering management questions 1 and 2 (in box at left); answers to management questions 3 and 4 are available to view in Appendix A. This chapter presents climate projections for the Sonoran Desert, MAPSS results for projected vegetation change linked to the climate projections, and climate change exposure and vulnerability results for the REA conservation elements. Although three different future climate projections were investigated, only the ECHAM5-driven RegCM3 climate projections were selected to evaluate potential impact on the various conservation elements. ECHAM5 is the fifth generation of the ECHAM Global Circulation Model (GCM) developed at the Max Planck Institute (Hamburg, Germany) and it has been identified as one of the better models to simulate natural climate variability (Mote et al. 2010, Garfin et al.

2010). The GCM-driven RegCM3 regional climate model projections were provided by S. Hostetler (U.S. Geological Survey) as representative of the North American Monsoon (Hostetler et al. 2011), which is important to Sonoran Desert vegetation dynamics.

5.4.1 Climate Projections

As explained in detail in Chapter 3, Methodology, the climate model data provided by Hostetler were averaged for two time periods (2015–2030 and 2045–2060), but only data from the 2045–2060 time period were used to evaluate the conservation elements, which are presented later in this section. For both temperature and precipitation results, water bodies were left as holes in the MAPSS model runs since no vegetation can be simulated over water. Climate projections surrounding water bodies are also considered less reliable because they create local moisture and turbulence conditions unrepresentative of the surrounding landscape, especially in semiarid areas.

Differences in temperature projections—average annual temperature (Figure 5-23), seasonal summer temperature (July–September; Figure 5-24), and winter temperature (January–March; Figure 5-25)—were calculated between historical (1968–1999) and future time periods (2015–2030 and 2045–2060) as simulated by the ECHAM5-driven RegCM3 model. Results show that the ecoregion is expected to undergo general warming over the entire region with a > 2° Celsius increase by 2060 in some locations, particularly in the southwestern portion of the ecoregion. Average summer temperatures are expected to increase, but greater increases are projected to occur during the winter months. This temperature increase is somewhat less than another recent projected modeled increase of 2.5°–3.0° Celsius for the region by Abatzoglou et al. (2011), who used an ensemble of 13 GCMs; these authors also projected an increase in the number of frost-free days and an increase in the length of the frost-free season.

Average Annual Temperature

PRISM 1968-1999

2015-2030

2045-2060

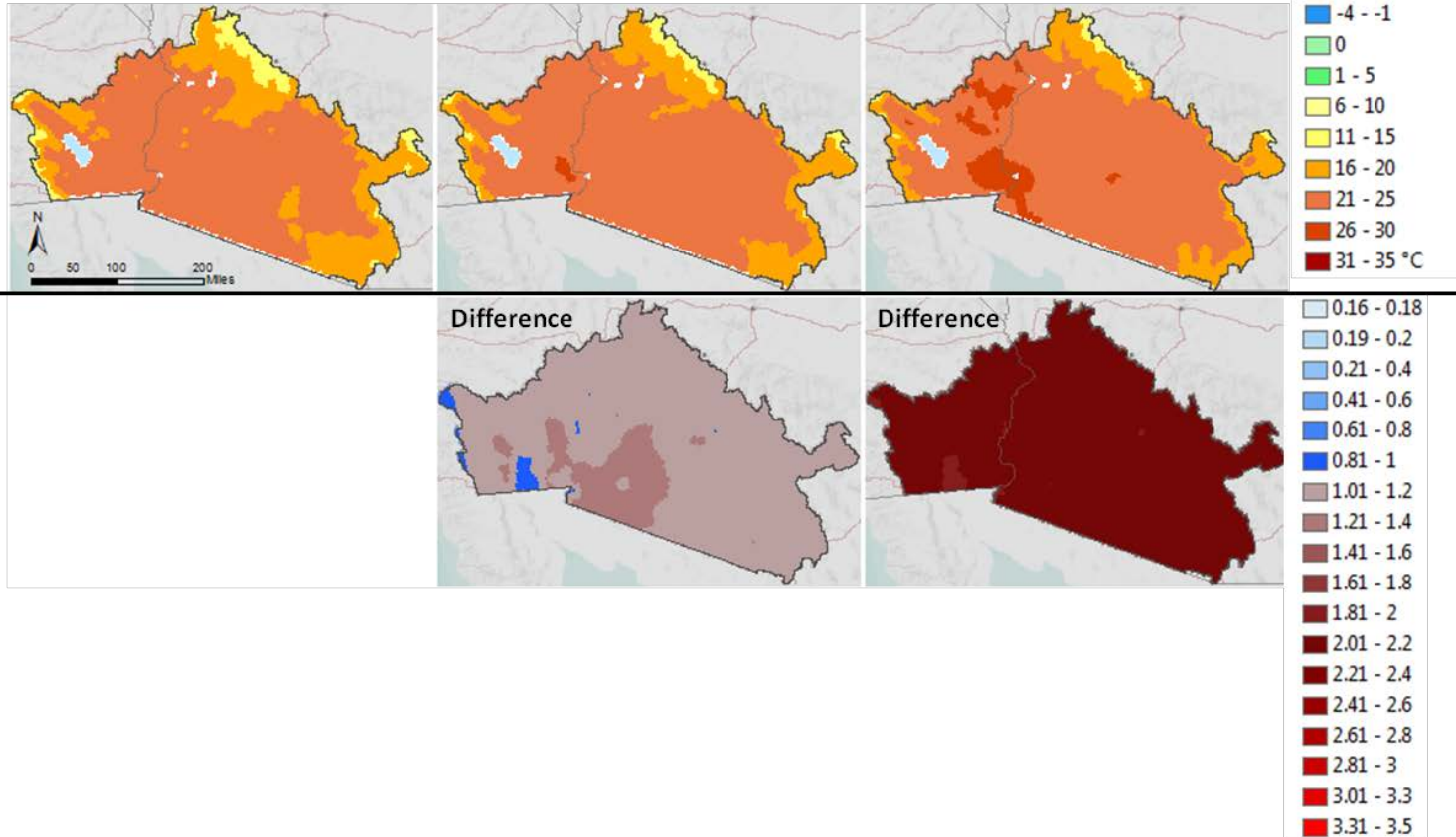


Figure 5-23. Map results for change in raw average annual temperature. Top Row: 1) Observed average annual temperature from PRISM averaged over the historical period (1968–1999 baseline) for the Sonoran Desert ecoregion.; 2-3) Bias-corrected future temperature using the ECHAM5-driven RegCM3 regional climate model deltas modifying the PRISM baseline (1) and averaged for two future time periods. Bottom row: Simulated ECHAM5-driven RegCM3 regional climate model differences between historical (1968–1999) and future (2015–2030; 2045–2060) average annual temperature. All colors on the difference maps are warmer than historic. Note: Bias correction was applied to the climate model results for more realistic climate input to the vegetation model. Future climate projections (top row 2-3) were generated by calculating the differences between future and historical temperature values simulated by RegCM3 (bottom row) and adding them to the historical PRISM baseline (top row).

Average Summer Temperature

PRISM 1968-1999

2015-2030

2045-2060

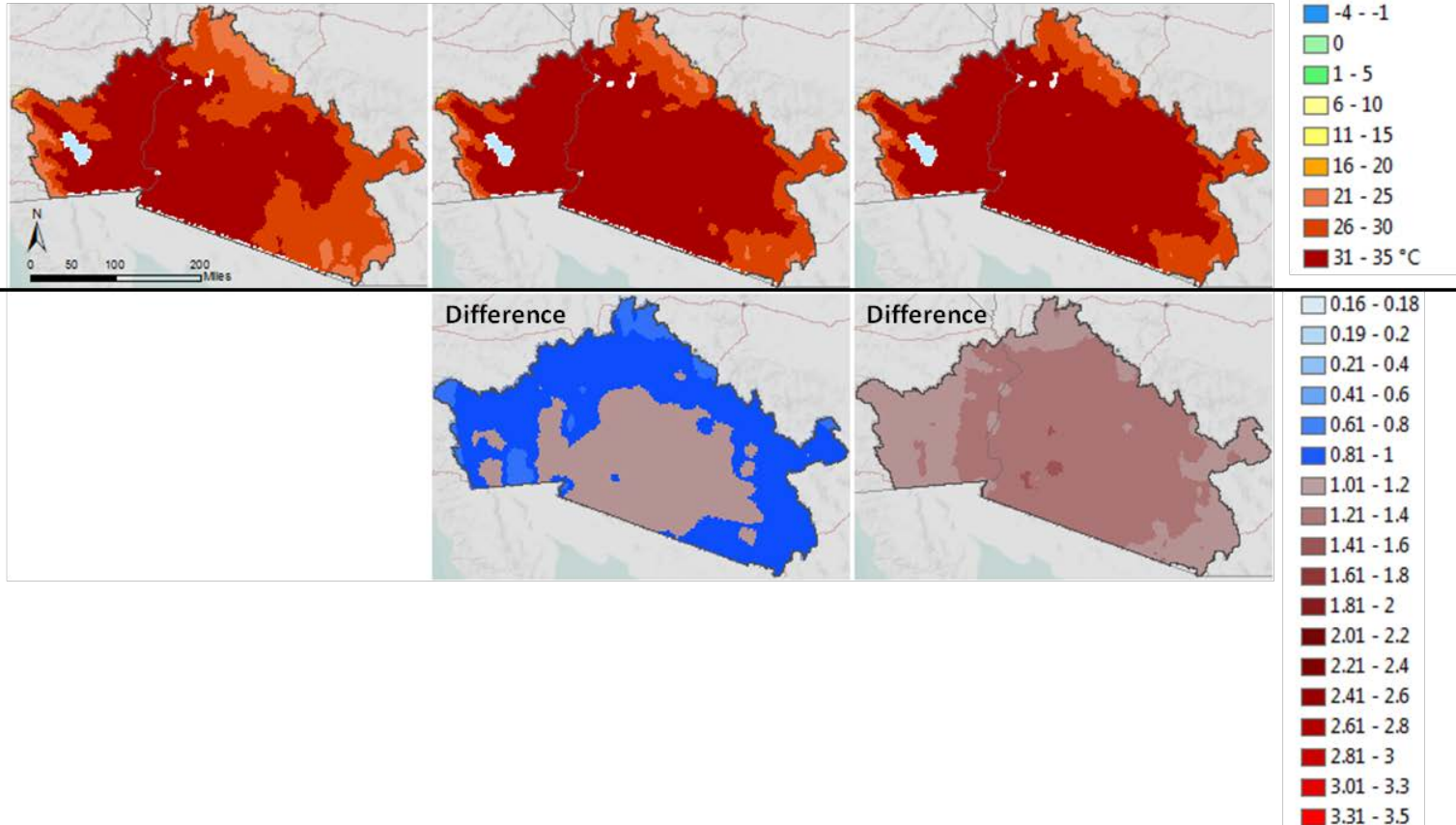


Figure 5-24. Map results for change in raw average summer temperature. Top Row: 1) Observed average summer (July–September) temperature from PRISM averaged over the historical period (1968–1999 baseline) for the Sonoran Desert ecoregion.; 2-3) Bias-corrected future summer temperature using the ECHAM5-driven RegCM3 regional climate model deltas modifying the PRISM baseline (1), and averaged for two future time periods. Bottom row: Simulated ECHAM5-driven RegCM3 regional climate model differences between historical (1968–1999) and future (2015–2030; 2045–2060) average summer temperature. All colors on the difference maps are warmer than historic. Note: Bias correction was applied to the climate model results for more realistic climate input to the vegetation model. Future climate projections (top row 2-3) were generated by calculating the differences between future and historical temperature values simulated by RegCM3 (bottom row) and adding them to the historical PRISM baseline (top row).

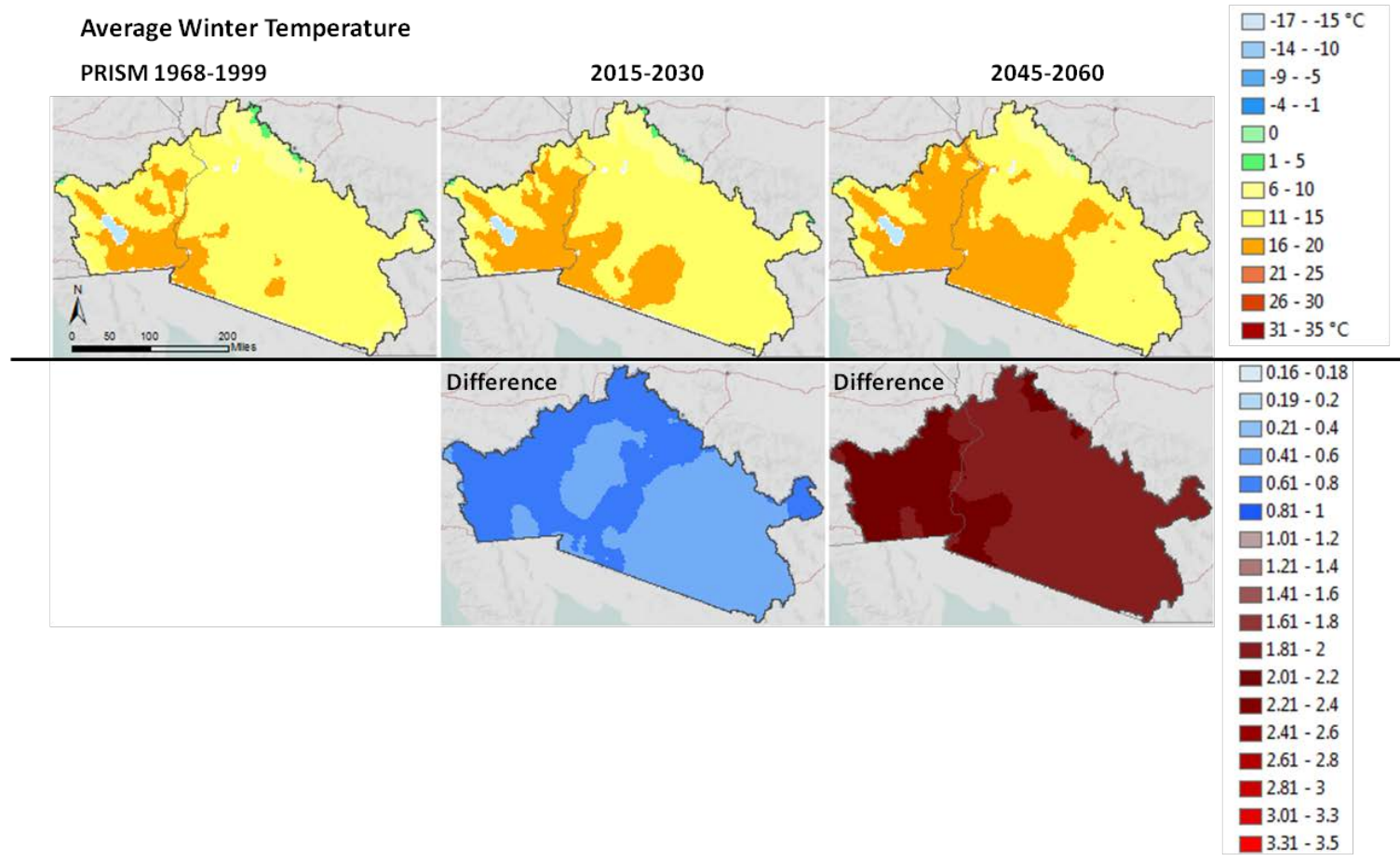


Figure 5-25. Map results for change in raw average winter temperature. Top Row: 1) Observed average winter (January–March) temperature from PRISM averaged over the historical period (1968–1999 baseline) for the Sonoran Desert ecoregion; 2-3) Bias-corrected future winter temperature using the ECHAM5-driven RegCM3 regional climate model deltas modifying the PRISM baseline (1), and averaged for two future time periods. Bottom row: Simulated ECHAM5-driven RegCM3 regional climate model differences between historical (1968–1999) and future (2015–2030; 2045–2060) average winter temperature. All colors on the difference maps are warmer than historic. Note: Bias correction was applied to the climate model results for more realistic climate input to the vegetation model. Future climate projections (top row 2-3) were generated by calculating the differences between future and historical temperature values simulated by RegCM3 (bottom row) and adding them to the historical PRISM baseline (top row).

It is generally accepted that climate models are less reliable in simulating precipitation than temperature because of field recording difficulties, scarcity of observations, large uncertainty in cloud generation, creating difficulties in model calibration. RegCM3 projections show significant declines in annual precipitation during the first time period with severe drought occurring in some areas (Graph, Figure 5-26, and Figure 5-27). Over the 2045–2060 timeframe, precipitation is projected to slightly increase over historical levels in parts of the eastern portion of the ecoregion, particularly during the fall (Oct–Dec). In contrast, Abatzoglou et al. (2011) predicted 20% drier conditions in November–March at mid-century (Abatzoglou et al 2011). The western region may remain drier than the historical period but not as dry as during the 2015–2030 time window.

Average summer precipitation (Figure 5-28) showed slightly more spatial variability than winter precipitation (Figure 5-29), especially during the 2045–2060 timeframe, even though both seasons tended to forecast drier conditions overall. Seager et al. (2007), using the ensemble mean of 19 GCMs (from the Intergovernmental Panel on Climate Change Assessment), looked at the difference between projected precipitation and evaporation in the Southwest region and warned of future droughts more intense than those recorded during the Dust Bowl of the 1930s and in the U.S. later during the 1950s. The degree of spatial and seasonal variation remains large, even when considering multi-model means. Historical records of precipitation show large natural variability and sensitivity to circulation patterns based on sea-surface temperature (e.g., El Niño Southern Oscillation). Such natural climate variability and its impacts have been well documented, but the understanding of the causes of shifts in circulation remains limited and thus difficult to include in climate models. With continuing natural variability in precipitation patterns, future patterns of change will be complex. However, there is general agreement that precipitation will decrease over much of the subtropics. In all of these systems, cloud formation and wind patterns are areas of uncertainty in model structure.

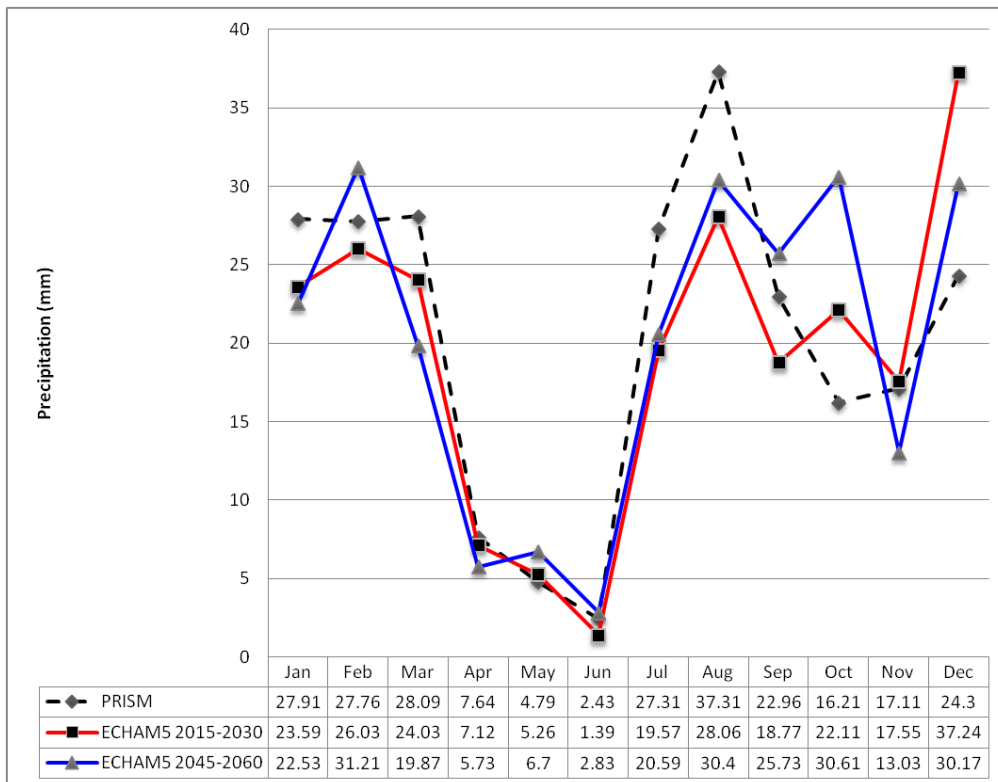


Figure 5-26. Monthly precipitation for historical conditions (PRISM historical precipitation averaged over the 1968–1999 time period) and for two future time periods (monthly precipitation averaged over the 2015–2013 and the 2045–2060 time period) simulated by the RegCM3 regional climate model with ECHAM5 boundary.

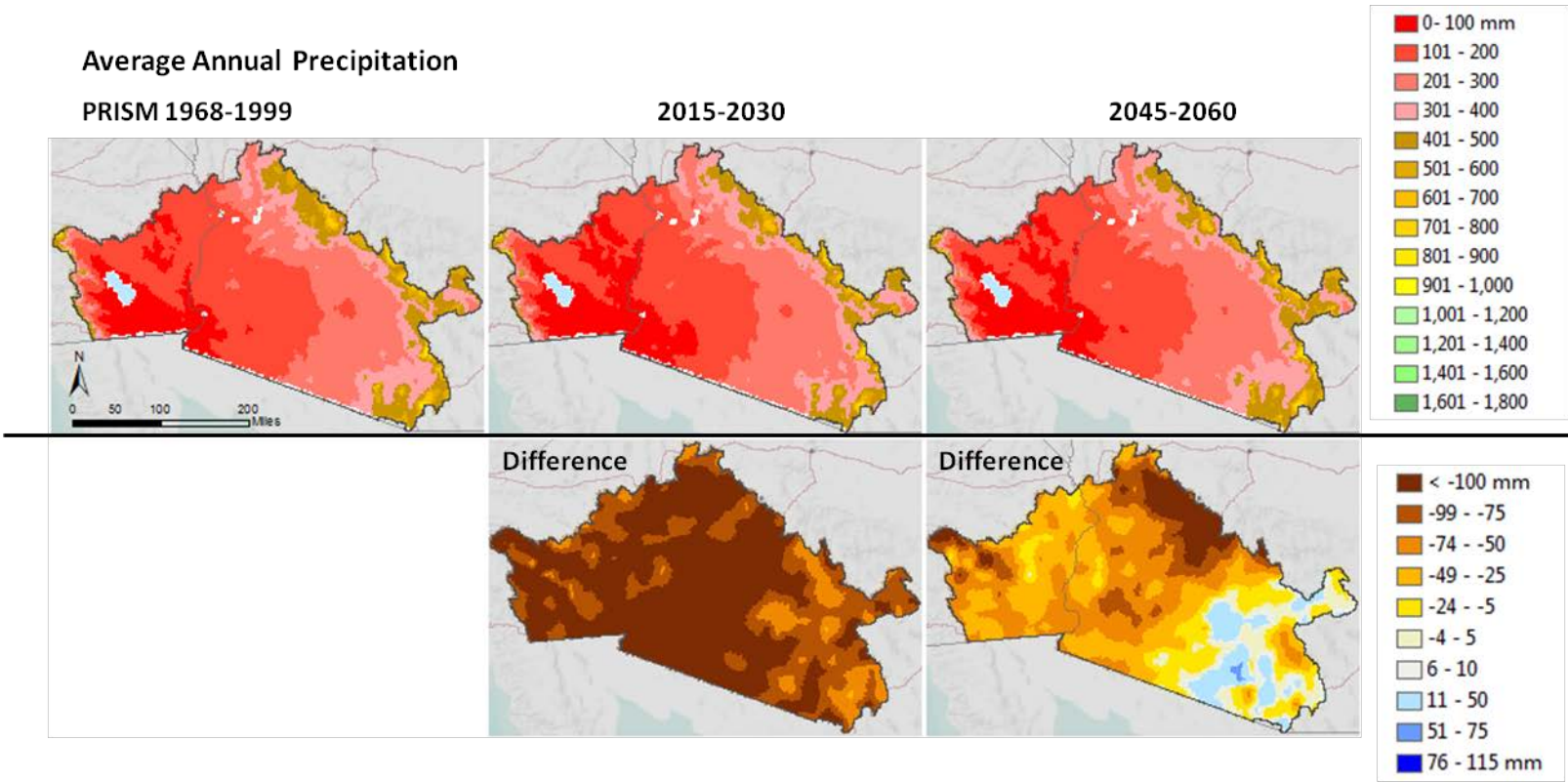


Figure 5-27. Map results for change in average annual precipitation. Top Row: 1) Observed average annual precipitation from PRISM averaged over the historical period (1968–1999 baseline) for the Sonoran Desert ecoregion.; 2-3) Bias-corrected future precipitation using the ECHAM5-driven RegCM3 regional climate model deltas modifying the PRISM baseline (1), and averaged for two future time periods. Bottom row: Simulated ECHAM5-driven RegCM3 regional climate model differences between historical (1968–1999) and future (2015–2030; 2045–2060) average annual precipitation. For the difference maps, brown color tones represent drier conditions and blue colors represent wetter conditions. Note: There was a large bias in the RegCM3 simulations of historical precipitation for this region. Consequently, the climate model results were bias-corrected to provide more realistic climate input to the vegetation model. Future climate projections (top row 2-3) were generated by calculating the ratios between future and historical precipitation values simulated by RegCM3 and multiplying them by the historical PRISM baseline.

Average Summer Precipitation

PRISM 1968-1999

2015-2030

2045-2060

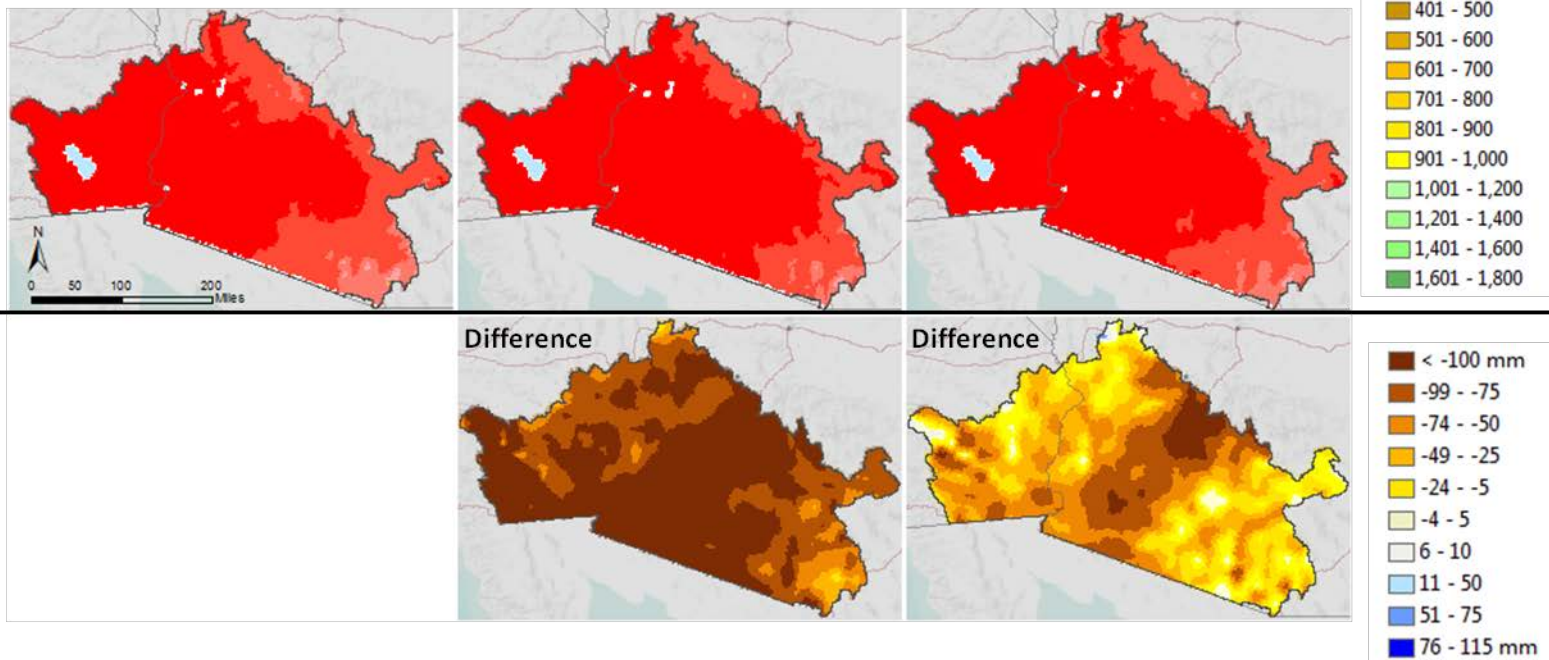


Figure 5-28. Map results for change in average annual summer precipitation. Top Row: 1) Observed summer precipitation (July–September) from PRISM averaged over the historical period (1968–1999 baseline) for the Sonoran Desert ecoregion.; 2-3) Bias-corrected future precipitation using the ECHAM5-driven RegCM3 regional climate model deltas modifying the PRISM baseline (1), and averaged for two future time periods. Bottom row: Simulated ECHAM5-driven RegCM3 regional climate model differences between historical (1968–1999) and future (2015–2030; 2045–2060) average summer precipitation. In difference maps, brown colors represent drier conditions and blue colors represent wetter conditions. Note: There was a large bias in the RegCM3 simulations of historical precipitation for this region. Consequently, the climate model results were bias corrected to provide more realistic climate input to the vegetation model. Future climate projections (top row 2-3) were generated by calculating the ratios between future and historical precipitation values simulated by RegCM3 and multiplying them by the historical PRISM baseline.

Average Winter Precipitation

PRISM 1968-1999

2015-2030

2045-2060

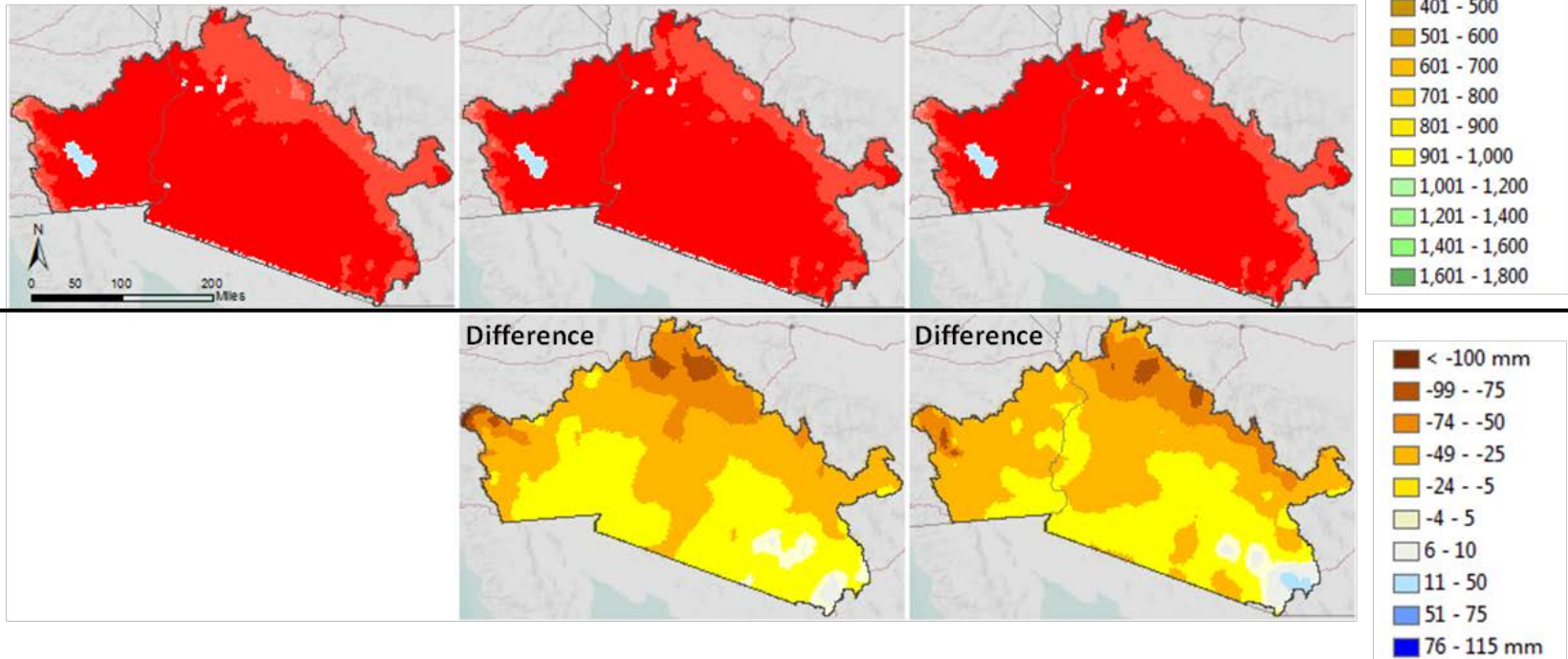


Figure 5-29. Map results for change in average annual winter precipitation. Top Row: 1) Observed winter precipitation (January–March) from PRISM averaged over the historical period (1968–1999 baseline) for the Sonoran Desert ecoregion.; 2-3) Bias-corrected future precipitation using the ECHAM5-driven RegCM3 regional climate model deltas modifying the PRISM baseline (1), and averaged for two future time periods. Bottom row: Simulated ECHAM5-driven RegCM3 regional climate model differences between historical (1968–1999) and future (2015–2030; 2045–2060) average winter precipitation. For the difference maps, brown color tones represent drier conditions and blue colors represent wetter conditions. Note: There was a large bias in the RegCM3 simulations of historical precipitation for this region. Consequently, the climate model results were bias corrected to provide more realistic climate input to the vegetation model. Future climate projections (top row 2-3) were generated by calculating the ratios between future and historical precipitation values simulated by RegCM3 and multiplying them by the historical PRISM baseline.

5.4.1.1 MAPSS Modeling Results

Four different MAPSS model variables (see Chapter 3 Methods) were provided for the REA—Leaf Area Index (LAI), Potential Evapotranspiration, Runoff, and Change in Vegetation cover. Simulated LAI slightly declined overall in most areas, suggesting a decline in water availability caused canopy thinning and/or a shift to sparser, more drought-resistant vegetation. Because the biogeography model (MAPSS) relies on fixed LAI thresholds to determine vegetation types, some shifts in vegetation cover were simulated (Figure 5-30). Only a few areas at higher elevations (where current vegetation is limited by low temperatures and not by water availability) displayed small increases in LAI (light grey-green pixels on the difference maps). An increase in Potential Evapotranspiration (PET) confirmed an overall drying trend concurrent with a decline in plant growth over most of the ecoregion (green areas on the map). Only at higher elevations are there signs of increased productivity where cooler temperatures reduce the drying effect (Figure 5-31). Surface runoff showed a slight increase over the near term—with less vegetation and as the soil surface became drier and less permeable to rainfall—and a slight decrease over the 2045–2060 time frame as more moisture penetrated the soil profile (Figure 5-32). Mountainous areas in the eastern portion of the ecoregion showed the greatest decline in runoff indicating a greater use of available water as temperatures rise.

One of the main projections from the MAPSS model is a potential shift in major vegetation types through time based on changes in plant functional groups. MAPSS uses the historical climate baseline (generated by the PRISM model) to predict the types of vegetation that would be supported under the given set of climate and soil conditions without human influence (see Chapter 3, Methods, Climate Modeling for more details). MAPSS does not take into account human management of natural landscapes or its long term legacy (e.g. water management, logging, grazing, etc.). It only uses climate and soil data to simulate potential vegetation cover. With a long history of human use in the ecoregion, the MAPSS historical simulation should not be expected to reflect exactly what is on the ground today.

Considerable change in vegetation is predicted between 1968–1999 and 2045–2060 (Table 5-3 and Figures 5-33 and 5-34). Since the MAPSS model is a static biogeography model, it is run independently for each of the two time periods. Therefore, results for an earlier period do not affect the outcome of a later run. Normally, any dry or wet periods have repercussions on the following year's vegetation response. In this case, the static vegetation model just simulates what potential vegetation the average climate can support during the period of interest.

Potential vegetation change simulated by the MAPSS biogeography model represents broad (global) vegetation classes based on climate and soil conditions (Figure 5-33 and 5-34). Three broad vegetation classes are depicted for the Sonoran Desert in the PRISM historical baseline time period: 1) desert subtropical in the Colorado Desert (western portion), 2) C₄ grasses in the eastern Sonoran Desert ecoregion, and 3) shrubland subtropical xeromorphic in the higher elevation areas surrounding the ecoregion (Figure 5-33, Table 5-3). Projections of change in these classes do not necessarily mean the identified potential vegetation type will establish during the time period of interest, only that the climate during that period is estimated to be suitable for the growth of that type. The projections may also indicate trends where vegetation mortality may occur if plants show no acclimation or adaptation potential. Some important regional vegetation classes, such as cacti in the Sonoran Desert, are not represented at all in the model because they photosynthesize in a different way from other plants (by utilizing CAM [or crassulacean acid metabolism] in photosynthesis). Many other factors not represented in the MAPSS model will affect future vegetation type such as fire, invasive species, dispersal ability, or recruitment.

The model projections show very dry annual and summer conditions during the 2020s, and slightly wetter conditions around 2050 (although still drier than historic mean). Winter precipitation increases slightly over both time periods. Winter and warm season rainfall influence germination and distribution of many Sonoran Desert plant species. With warmer, somewhat drier conditions, desert subtropical vegetation, such as creosotebush-white bursage in the Colorado Desert of California and southwestern Arizona, is projected to expand in the 2015–2030 time period, but then recede in 2045–2060 replaced by an expansion of semi-desert C₄ grasses (see Glossary). Even this drought resistant community has limits. Creosotebush is susceptible to prolonged drought and its distribution is correlated with winter precipitation (Marshall 1995, Munson et al. 2011). Munson et al. (2011), in a study of the effects of climate variability on Sonoran Desert vegetation communities over the last century, found that the cover of creosotebush decreased with increased aridity and a decrease in winter precipitation (below 135 mm). They also noted that in years with high temperatures the cover of foothills paloverde and ocotillo decreased and cacti increased in the Arizona Upland. Recent drought in the early 2000s also caused nearly complete mortality of white bursage and other shrubs in the California portion of the Sonoran and Mojave Deserts (McAuliffe et al 2010).

The interpretation of the projected expansion of C₄ grasses is more complex. C₃C₄ dominance is a function of the inter-relationship of seasonal precipitation, growing season temperature, and atmospheric CO₂ levels (Ehleringer 2005). C₃ grasses (which include native grasses as well as invasive species such as red brome) dominate in a region where summers are dry and most precipitation falls in winter and early spring (such as in the Mojave Desert and western Sonoran Desert), but areas with summer precipitation (like the eastern Sonoran Desert) favor C₄ grasses (Ehleringer 2005). Projected temperature increases with climate change are predicted to favor warm-season C₄ grasses (Ehleringer et al. 1997, Morgan et al. 2011). Cool season C₃ grasses are expected to benefit from rising CO₂ levels (Ehleringer et al. 1997, Morgan et al. 2011), if reduced winter precipitation does not lead to a decline in their distribution (Ehleringer 2005). On the other hand, increasing CO₂ is expected to have a fertilizing effect and to increase water use efficiency, which may offset the possible declines in C₃ grasses from reduced winter precipitation (Morgan et al. 2011).

Besides the changes in the distribution of grasses, the MAPSS results project an increase in shrub savanna subtropical mixed vegetation (Table 5-3), represented by mesquite savanna and juniper-oak savanna found in the transition to higher elevation ecoregions surrounding the Sonoran Desert. Chaparral, also found in these transitional ecotones (both maritime and interior) and on some interior mountain ranges, shows no change in the model results (shrubland subtropical Mediterranean, Table 5-3). Eight other vegetation types, in addition to desert subtropical vegetation mentioned earlier, declined in area by 2045–2060 (Table 5-3).

Other investigators have found warming trends in winter and spring, decreased frequency of freezing temperatures, lengthening of the frost free season and increased minimum temperatures in the Sonoran Desert (Abatzoglou et al. 2011). With warming expected to continue at faster rates throughout the 21st century along with a possible decline in the summer monsoon, biotic interactions and competition between shallow- and deep-rooted species, photosynthetically heat-adapted species, and invasive grasses will drive the reconfiguration of what is currently known as the Sonoran Desert. Potential ecological responses may include increased incidence of fire, expansion of invasive species, loss of woody plant cover, and changes in the regional boundaries of the Sonoran Desert ecoregion. The ecoregion may contract in the south-east and expand northward, eastward, and upward in elevation. The distributions of characteristic plant species within Sonoran Desert ecosystems may also change, including a possible decrease in the iconic giant saguaro (Weis and Overpeck 2005, Ryan and Archer 2008).

In summary, land managers should begin to prepare for changes in the known ecoregions, shifts in vegetation composition, diversity and growth, losses in net primary production, intensification of the hydrologic cycle (more intense runoff), reduced streamflow and native fish diversity, increased soil erosion, increases in nonnative species, and increased frequency and intensity of fire (Archer and Predick 2008).

Leaf Area Index

PRISM 1968-1999

2015-2030

2045-2060

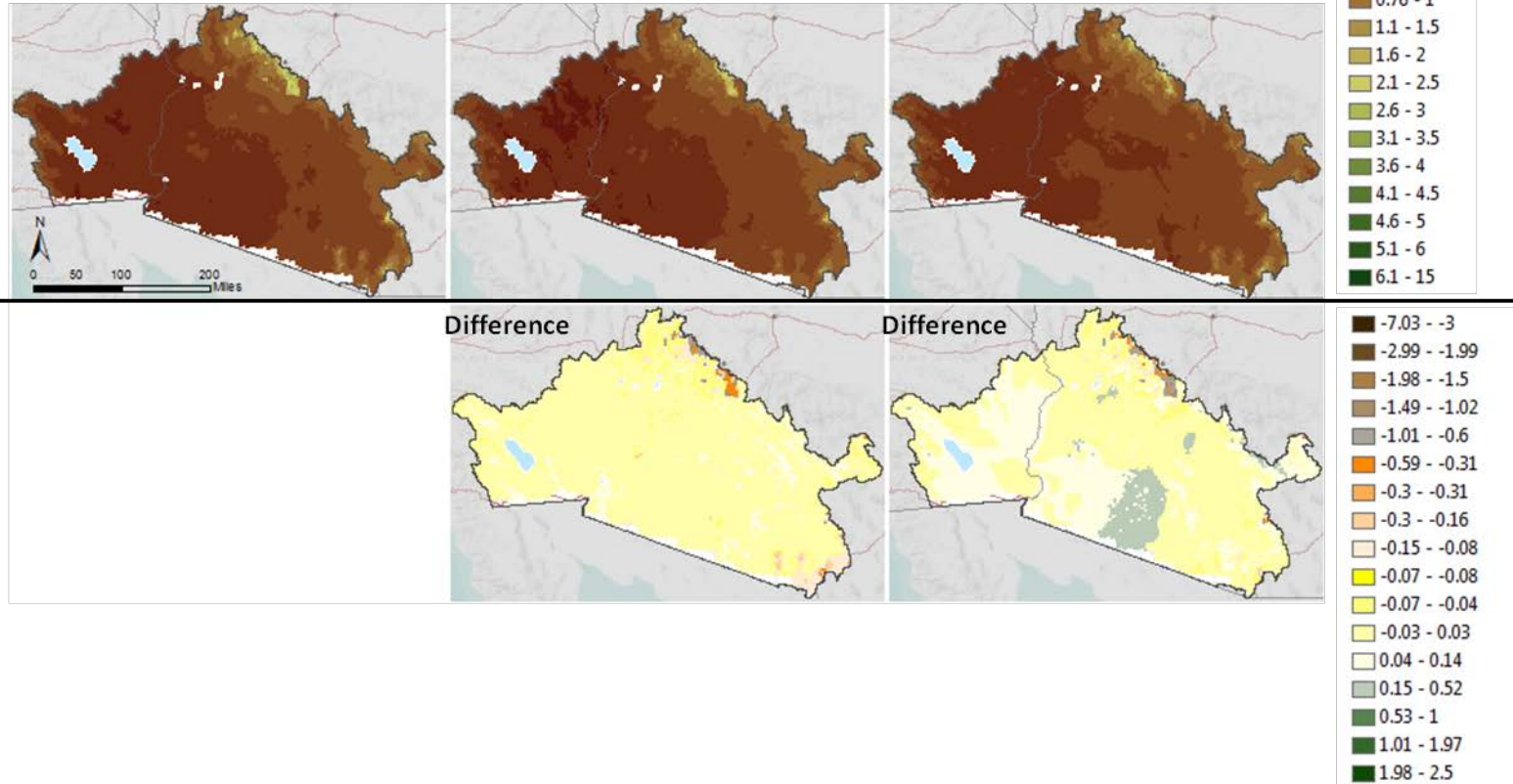


Figure 5-30. Leaf Area Index (LAI) simulated by the static biogeography MAPSS model for the Sonoran Desert ecoregion for historical and future (2015–2030 and 2045–2060) time periods. The top row shows LAI values and the bottom row differences between historical and future projections.

Potential Evapotranspiration

PRISM 1968-1999

2015-2030

2045-2060

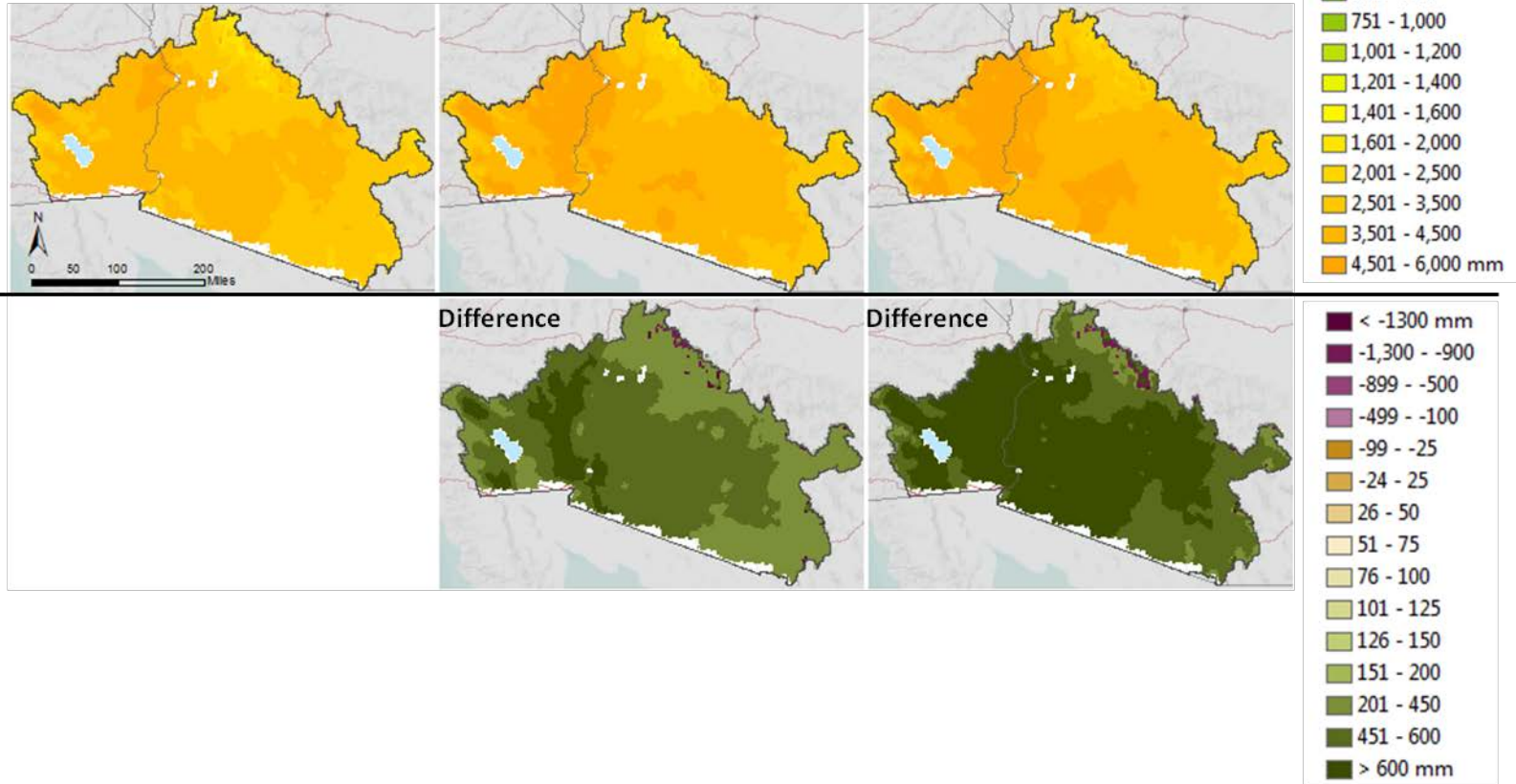


Figure 5-31. Potential evapotranspiration (PET) simulated by the static biogeography MAPSS model for the Sonoran Desert ecoregion for historical and future (2015–2030 and 2045–2060) time periods. The top row shows LAI values and the bottom row differences between historical and future projections.

Runoff

PRISM 1968-1999

2015-2030

2045-2060

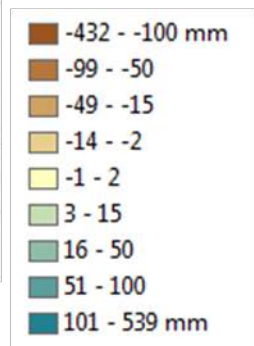
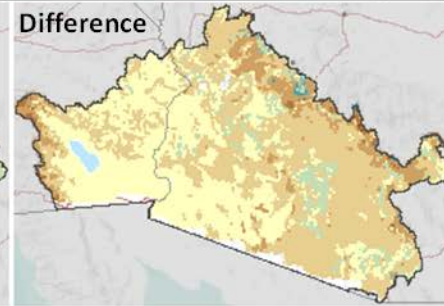
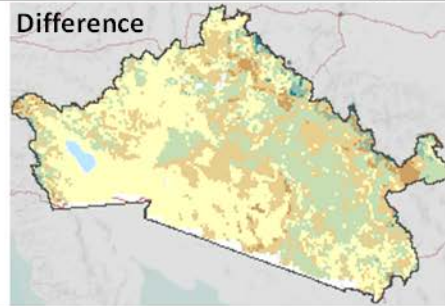
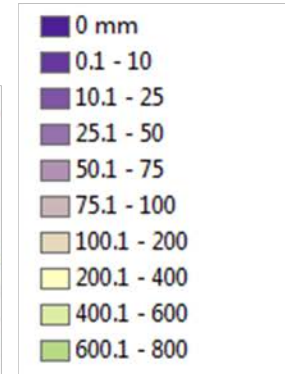
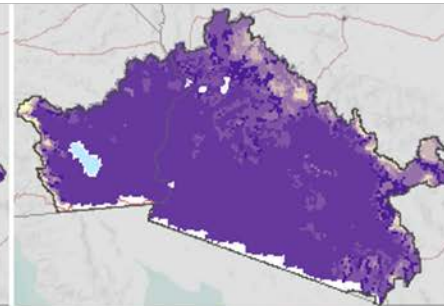
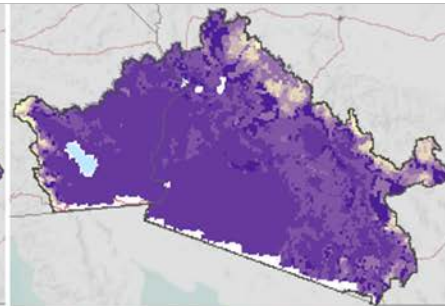
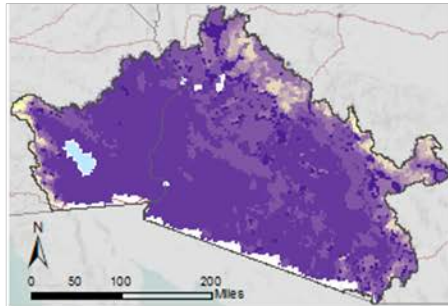


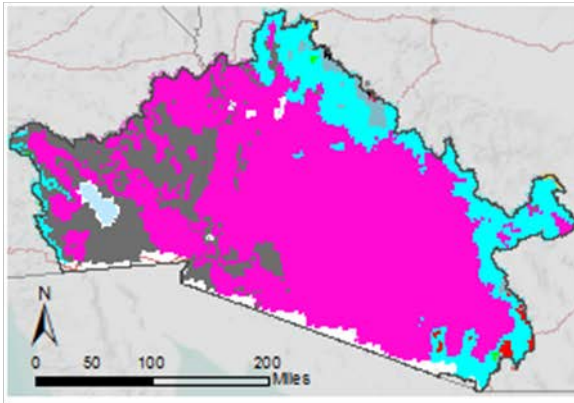
Figure 5-32. Surface runoff simulated by the static biogeography MAPSS model for the Sonoran Desert ecoregion for historical and future (2015–2030 and 2045–2060) time periods. The top row shows LAI values and the bottom row differences between historical and future projections.

Table 5-3. Change (in 1000s of acres) in major vegetation type as simulated by the biogeography MAPSS model for the Sonoran Desert ecoregion.

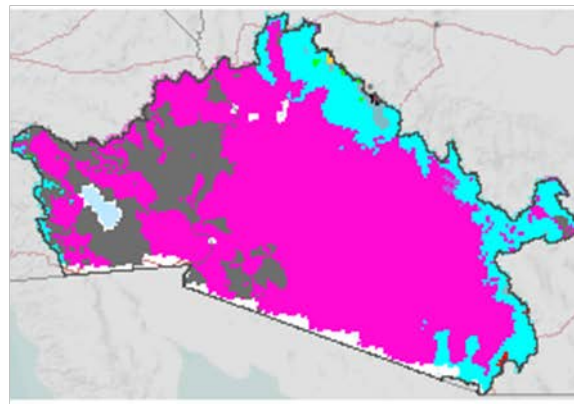
PRISM	2045 to 2060	Potential Change (ac)	Vegetation Type	Example Species
593	253	-340	Tree Savanna Mixed Warm	oak savanna
24	0	-24	Tree Savanna Evergreen Needle Continental	ponderosa pine
40	4	-36	Tree Savanna PJ Continental	pinyon pine, western juniper
4	0	-4	Tree Savanna PJ Maritime	California oak and coastal sage, west Sonoran boundary
40	20	-20	Shrub Savanna Evergreen	sagebrush, saltbrush
178	435	257	Shrub Savanna Subtropical Mixed	mesquite savanna, juniper-oak savanna
5,903	5,851	-51	Shrubland Subtropical Xeromorphic	oak-juniper woodland, mountain mahogany-oak scrub
47	47	0	Shrubland Subtropical Mediterranean	chaparral
16	0	-16	Grass MidC3C4	wheatgrass, ricegrass
75	0	-75	Grass ShortC3C4	bluegrass, grama
8	759	751	Grass ShortC4	muhly grass, blue grama
22,350	26,687	4,337	Grass SemiDesertC4	galleta, grama
5,365	585	-4,780	Desert Subtropical	creosotebush, palo verde

Change in Vegetation

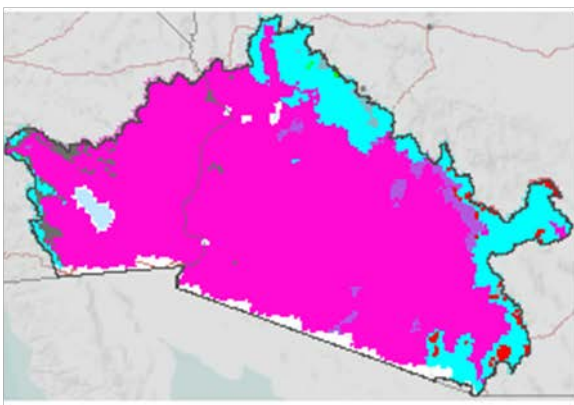
PRISM 1968-1999



2015-2030

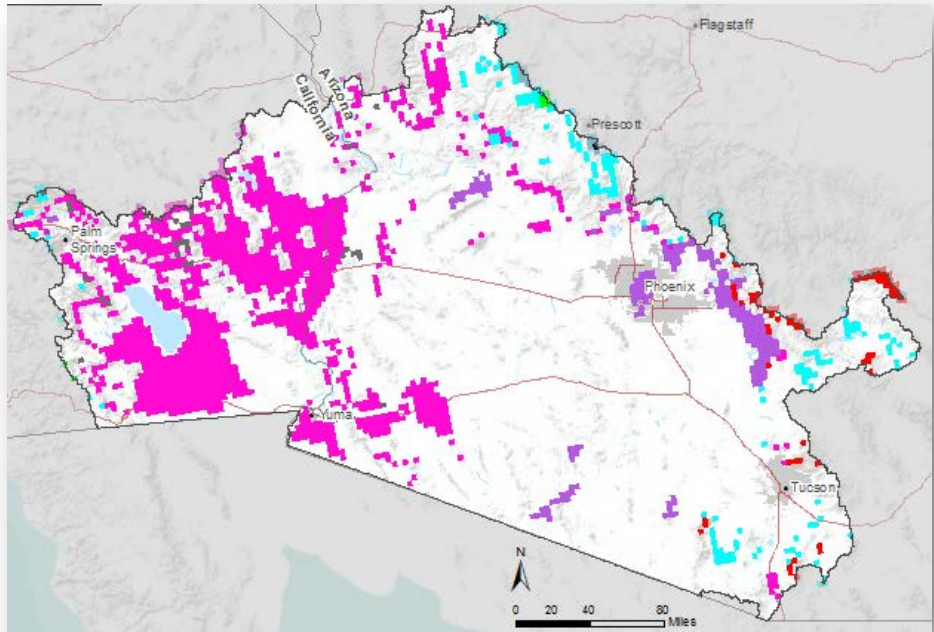


2045-2060



- Tree savanna mixed warm (EN)
- Tree savanna evergreen needle continental
- Tree savanna PJ continental
- Tree savanna PJ maritime
- Shrub savanna evergreen micro
- Shrub savanna subtropical mixed
- Shrubland subtropical xeromorphic
- Shrubland subtropical mediterranean
- Grass mid C3/C4
- Grass short C3/C4
- Grass short C4
- Grass semi desert C4
- Desert subtropical

Figure 5-33. Vegetation distribution simulated by the MAPSS biogeography model for the Sonoran Desert ecoregion over the historical period (1968–1999) and two future time periods (2015–2030 and 2045–2060).



- Tree savanna mixed warm (EN)
- Tree savanna evergreen needle continental
- Tree savanna PJ continental
- Tree savanna PJ maritime
- Shrub savanna evergreen micro
- Shrub savanna subtropical mixed
- Shrubland subtropical xeromorphic
- Shrubland subtropical mediterranean
- Grass mid C3/C4
- Grass short C3/C4
- Grass short C4
- Grass semi desert C4
- Desert subtropical

Figure 5-34. Areas of vegetation change (showing just the pixels that changed) between the historical period (1968–1999) and one future period (2045–2060) based on the MAPSS biogeography model for the Sonoran Desert ecoregion.

5.4.1.2 Uncertainty in Climate Change Modeling

Uncertainty can be examined in different ways and from different perspectives. First, impacts models depend on the reliability of the climate data that they use. It is important to note that while climate projections diverge after 2040, models generally agree for the first half of the century and the choice of a particular climate model or scenario is less important if the management goal is limited to the next 2 or 3 decades. Beyond 2040, it becomes critical to rely upon experts who can select climate models based on less than perfect criteria. For example, it is common to choose climate models that best simulate past climate dynamics, particularly paying attention to the most important local climate feature (as was done for this REA with the choice of the RegCM3 model that recognizes the summer monsoon for the U.S. Southwest). Three GCMs driven by the RegCM3 regional model were analyzed for this project: ECHAM-5, GFDL and GENMOM. The data portal contains the results of each model, including associated MAPSS results; access at <http://www.blm.gov/wo/st/en/prog/more/climatechange.html>. Users can delve into these models to gain a deeper understanding of the range of potential results from various models.

Model verification is obviously impossible for future projections and one is reduced to putting one's confidence in the ability of climate models to reproduce faithfully past climatic changes. However, there is no guarantee that a model that reproduces the past well will simulate the future accurately. Current models include our current understanding of past climate dynamics that may change drastically as atmospheric and stratospheric composition change as well as the planet's albedo. General circulation models (GCMs) were designed to simulate the planet's climate and their results compare well to climate observations at the global scale. The accuracy of global models declines at the local scale due to their inherent coarse spatial resolution that averages diverse vegetation cover and complex topography so important to conservation practitioners. Downscaling techniques (statistical or dynamic) bring GCM results to the scale of concern, but their accuracy is limited to that of the original projection. Furthermore, feedbacks from the biosphere to the atmosphere continue to be woefully under-represented in global models and regional model feedbacks to the GCMs have not even been developed yet. The uncertainty of climate projections result from the imperfect knowledge of 1) initial conditions such as sea surface temperatures that are difficult to measure, 2) the levels of future anthropogenic emissions, which are unknowable since they are dependent on current and future political decisions and social choices, and finally 3) general system behavior (such as clouds and ice sheet melt) that continues to be the subject of basic climate research and that constitutes the "known unknowns" of the climate system. Finally, surprises such as the unexpected Larsen B ice shelf rapid collapse in Antarctica, one of the "unknown unknowns", also cause climate scientists to continually improve existing models. It is important to understand that as change occurs (e.g. ice free poles, glacier disappearance, new wind patterns, change in ocean currents), the basic assumptions at the core of the climate models may become obsolete, reminding us again that there is no assurance that a model that reproduces the past well is going to be reliable when projecting the future. Climate scientists learn constantly from every new observation and they update their models accordingly as new observations bring new knowledge. Moreover, the accuracy of the emission scenarios used by the Intergovernmental Panel on Climate Change (IPCC) depends entirely on political decisions and social choices that, by definition, are impossible to predict.

Extreme events (e.g. long, intense droughts, floods, and hurricanes) are also difficult to predict by climate models. Along with a greater risk of drought, there is an increased chance of intense precipitation and flooding due to the greater water-holding capacity of a warmer atmosphere such that both wet and dry extremes should become more severe. These extreme events, while unpredictable, are often what shape our landscapes. Past extreme events such as the drought of the 1930s that caused the Dust Bowl certainly affected natural ecosystems and human land use, but recently, records of extreme events have been increasing in the U.S. For example, the drought of 1999–2002 that spawned fires, dust storms, and pinyon pine mortality across the southwestern states may have been an indication of climate destabilization. These

extremes are consistent with what climate scientists have been expecting. Extreme events certainly pose a challenge to land managers who are typically more comfortable thinking about chronic linear change rather than abrupt and unpredictable change.

At the local scale, practitioners need to be aware of the uncertainty of climate baselines and projections due to: 1) the variable density of meteorological stations in or close to their area of concern and the length of records from these stations reducing the reliability of historical records; 2) the topographic complexity that can cause local decoupling from regional climatic trends (see next paragraph below); 3) the relative proximity of their sites to large terrain features that can affect local conditions and not be simulated well by climate models; 4) the proximity to water (stream or coast) and its importance for cooling influences and groundwater availability; 5) the influence of human activities in or near the conservation site (pollution levels and cloud condensation nuclei, fire ignition source, urban island heat effect); 6) the natural climate variability and the records of extreme events that, once known, can increase the understanding of ecosystem vulnerability to future climate disturbance.

There is inherent natural variability in the expression of climate (e.g. cold air drainage, inversions in deep valleys), which is often influenced by the complexity of the regional terrain. At a fine scale, this means localized climate refugia—narrow swales, moist draws, etc. Close examination of a reasonable resolution (30 m) digital elevation model (DEM) can provide some insight as to locations that are more likely to provide refugia (Figure 5-35). These sites are found at a much finer scale than the analytical grid of the climate change work. At a coarser level, places on the landscape in and around rugged terrain will experience higher natural levels of climate variability.

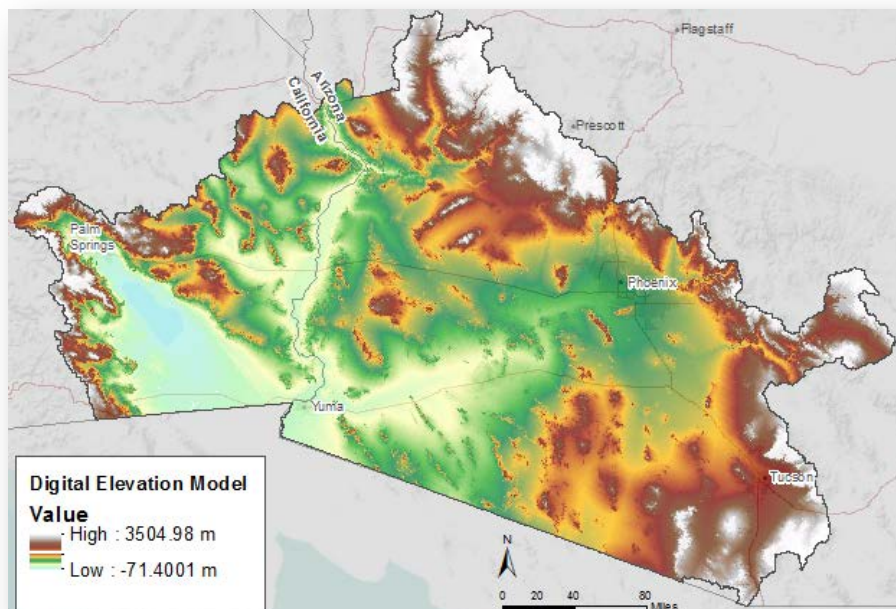


Figure 5-35. Digital elevation model (DEM) for the Sonoran Desert ecoregion

Calculating the pixel standard deviation of annual average temperature and annual average precipitation separately based on the PRISM historic data provides map products that highlight areas on the landscape that are prone to more variability for these primary climate variables (Figure 5-36). The natural variability of precipitation for this arid landscape is quite small at lower elevations, but the range of variability increases to a modest degree as elevation increases.

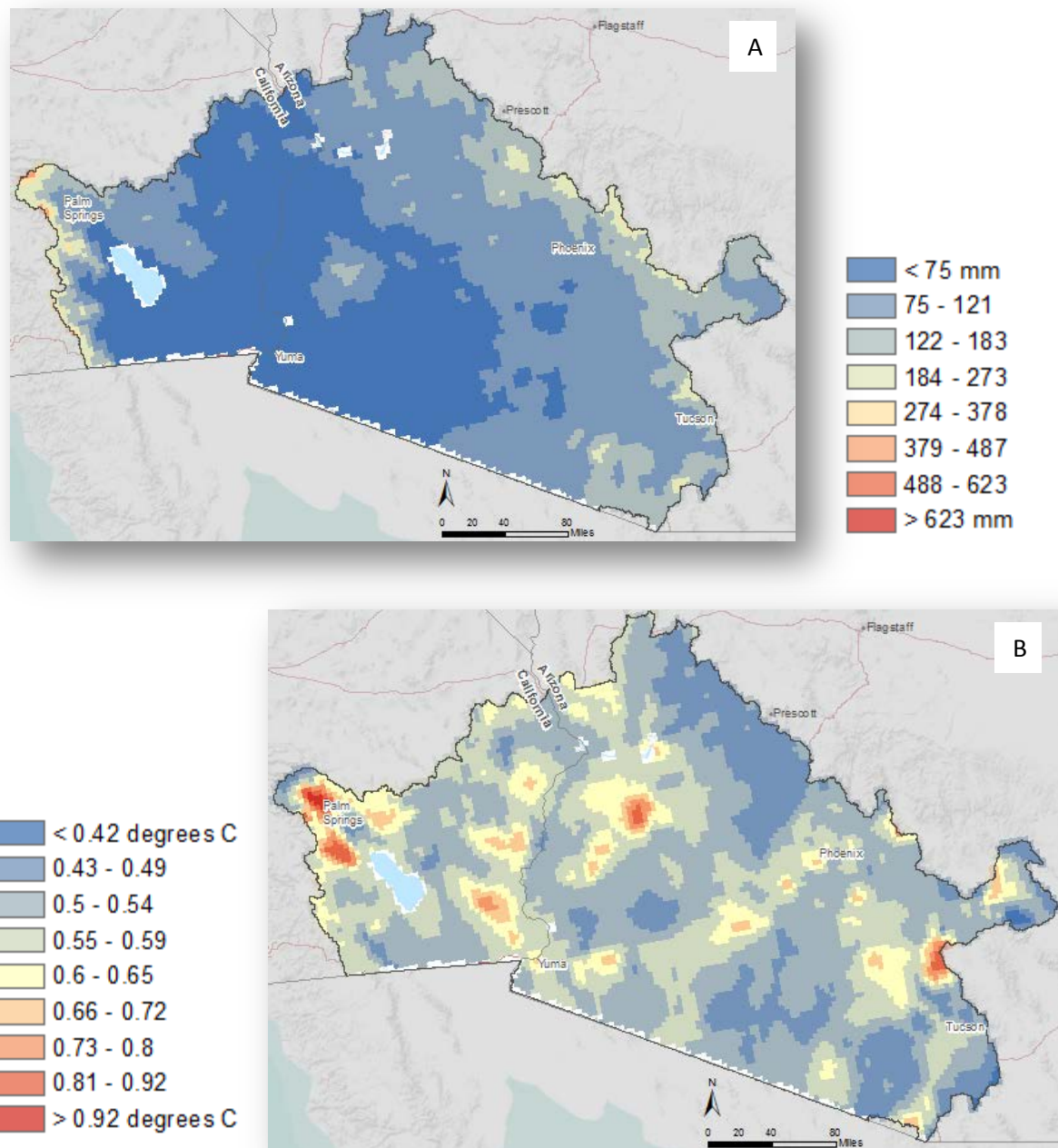


Figure 5-36. Uncertainty depicted as standard deviation of (A) precipitation and (B) temperature data from PRISM historic condition (1968–1999).

The range of variability is more pronounced for the temperature data. Here, the valleys express higher levels of temperature variability from year-to-year (areas that are orange). These areas are highly influenced by the close proximity of the various mountainous areas. These results allow us to infer that: 1) plants and animals living in areas with a naturally variable climate have likely evolved mechanisms to cope or adapt to that variability; and 2) climate forecasts in these areas will tend to be less reliable compared to locations where year to year variability is less pronounced.

5.4.1.3 Assessing Climate Change Exposure for Conservation Elements

To simplify the numerous future climate projections and MAPSS modeling results, a number of key findings from these analyses were assembled into an overall relative climate change map. The different classes of potential for climate change were then overlaid on the distributions of specific conservation elements to assess their relative exposure to climate change and to respond to four different climate-change-related management questions (MQ D6, J1, J2, and J3, see Table 2-1). The fuzzy model inputs included potential for summer temperature change and potential for winter temperature change averaged into a single factor, and change in precipitation, runoff, and vegetation change simulated by the MAPSS model (Figure 5-37). Direction of the change was not important—only its degree of departure from the historic baseline. Details regarding change in temperature by degrees or actual predicted changes in precipitation can easily be assessed from the additional datasets provided in the body of the text. The model logic stated that all 4 km x 4 km pixels with potential to change primary vegetation type get the highest change score while the rest of the landscape received an average value based on the combination of the other factors. Departure in temperature in either season dominated that intermediate product that is then averaged with the two water functions (purple box plus two gold boxes in the intermediate results in the logic model below). Appendix E presents quality of data sources and level of confidence in the overall model.

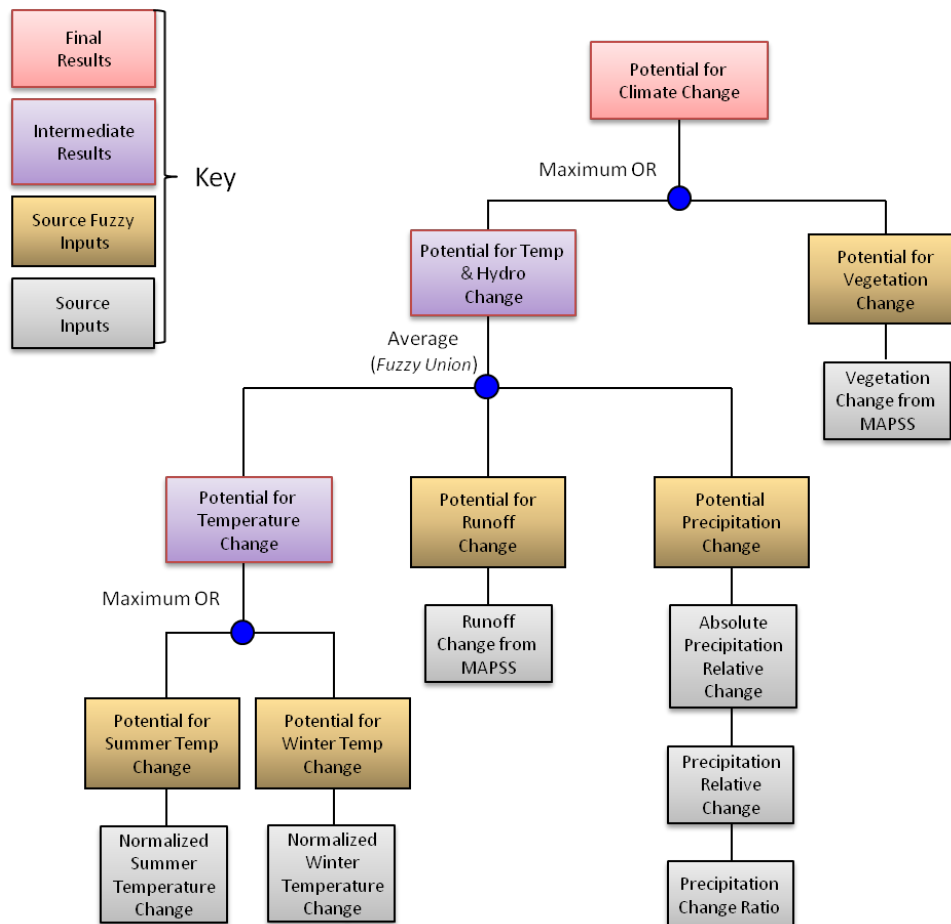


Figure 5-37. Fuzzy logic model for integrating climate change data to assess potential exposure of conservation elements to climate change in the Sonoran Desert ecoregion.

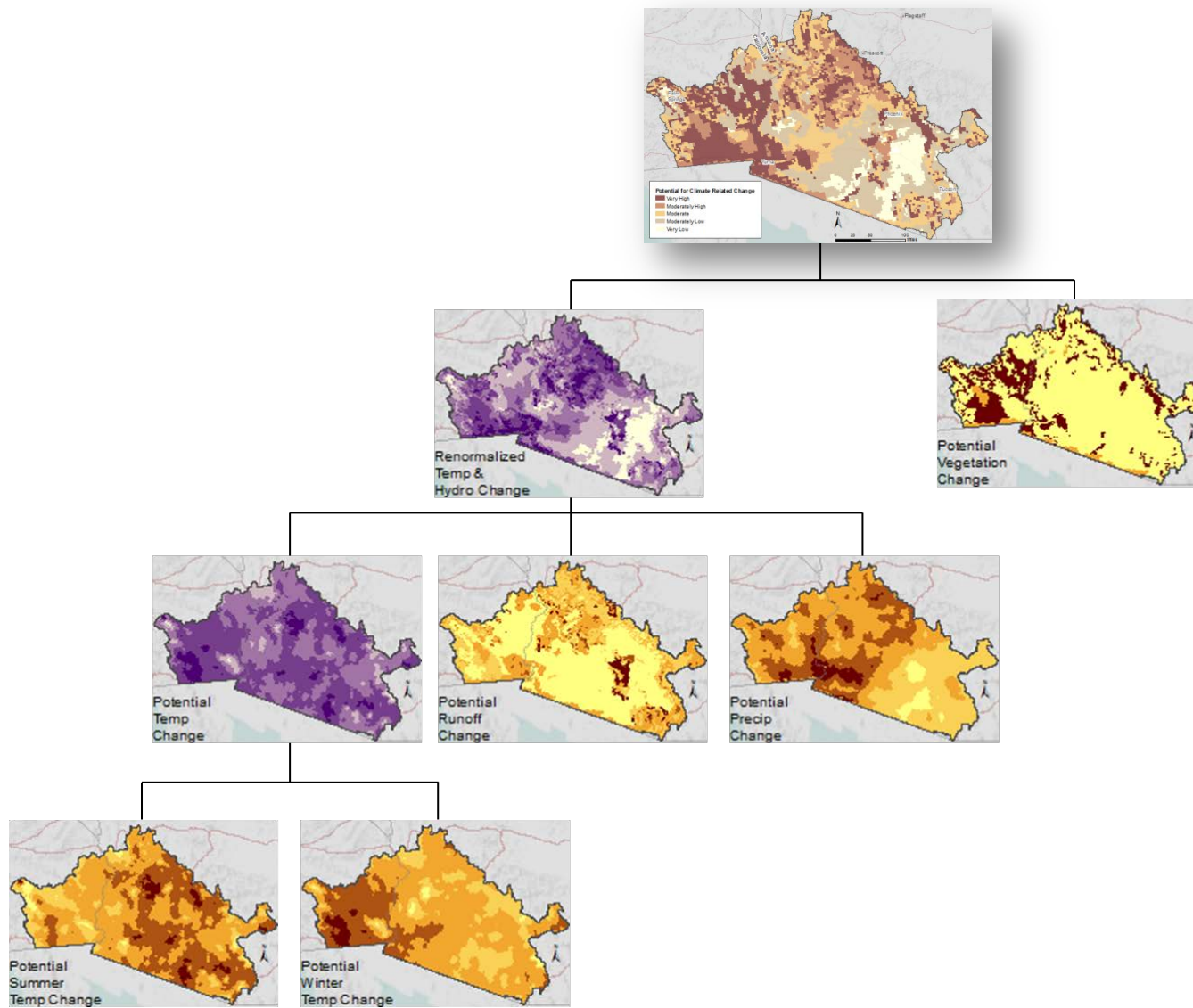


Figure 5-38. Map outputs for each step in the climate change fuzzy logic model for the Sonoran Desert ecoregion.

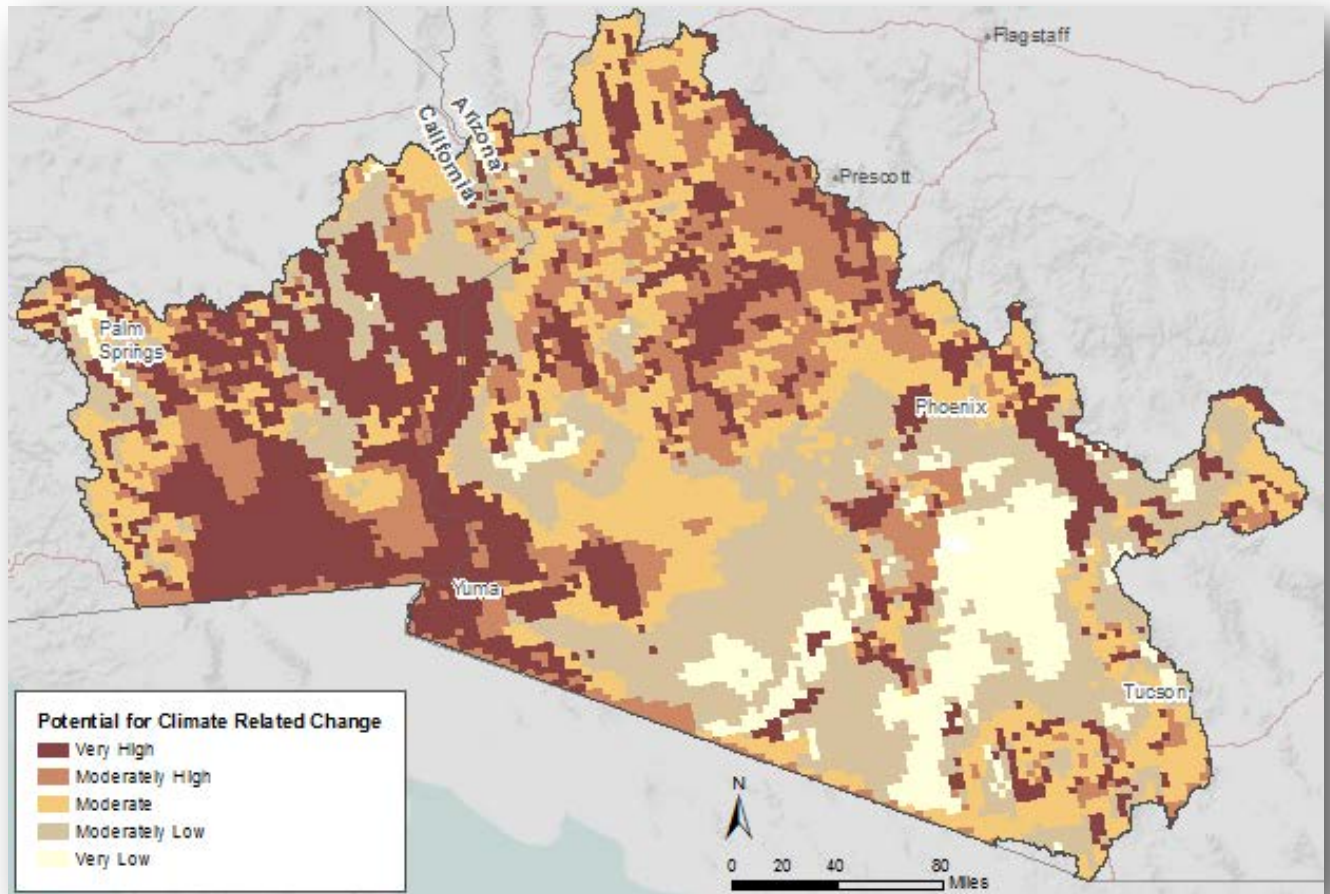


Figure 5-39. Final climate change potential map for the Sonoran Desert ecoregion. Fuzzy model inputs included potential for summer and winter temperature change averaged into a single factor and change in precipitation, runoff, and vegetation change simulated by the MAPSS model. Map shows five separate climate change exposure classes (Very High, High, Moderate, Moderately Low and Low) for the 2045–2060 time period.

Results from the fuzzy logic model show the contributions made by the various model components (Figure 5-38) to the final climate change potential map (Figure 5-39). Areas most likely to show the greatest changes are those that are predicted to change in their vegetation type or that scored high from a combination of the other factors.

The climate change model results, when overlaid with species' and vegetation communities' distribution maps, indicate the conservation elements' exposure to climate change. Exposure is just one aspect of ecosystem and species' vulnerability to climate change. Vulnerability is defined by the United Nations' Intergovernmental Panel on Climate Change (IPCC 2001) as...“(t)he degree to which a system is susceptible to, or unable to cope with, adverse effects of climate change, including climate variability and extremes. Vulnerability is a function of the character, magnitude, and rate of climate variation to which a system is exposed, [as well as] its sensitivity and its adaptive capacity.” See also the definition in Glick et al. (2011). The sensitivity of a species or system to climate change can be considered in terms of a “dose-response” relationship describing its exposure, resulting impacts, and its response (decline or adaptation, Füssel and Klein 2006). The development of vulnerability indices requires the implementation of species-specific indicators of sensitivity and species response or capacity to adapt, along with thresholds of impact that may

indicate subsequent species decline (Carter et al. 2007). Füssel (2007) notes that time must be factored in as well. Sensitivity represents immediate or short-term effects on a system or species, while resilience or adaptation must be considered over a longer time frame to assess the species' ability to maintain basic functions and possibly return to its original state. Although no readily-available metrics yet exist to quantitatively describe the vulnerability of an ecosystem or species to climate change (Füssel and Klein 2006, Adger 2006, Carter et al. 2007), the pressing need to identify vulnerable species and to manage for mitigation under various climate change scenarios has prompted the development of more qualitative approaches to project species' vulnerability (Glick et al. 2011, Young et al. 2011).

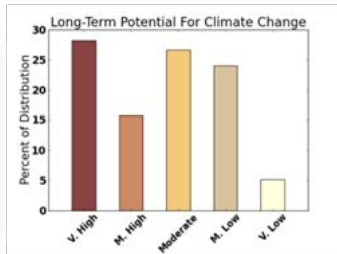
The REA climate change results presented here for individual conservation elements are modeled from available spatial data and focus on the exposure of species, habitats and sites to projected climate change. However, some non-spatial species sensitivity information was obtained for some of the REA wildlife conservation elements from a Climate Change Vulnerability Index (CCVI) developed for the Nevada/Mojave region (NNHP 2011). CCVI is a product of assessment teams employing literature review, professional judgment, and expert review through workshops (Young et al. 2011). In this CCVI, the range and abundance of eight of the 11 REA wildlife species conservation elements selected for the Sonoran Desert ecoregion (mule deer, desert bighorn, Lucy's warbler, southwestern willow flycatcher, Le Conte's thrasher, Bell's vireo, golden eagle, and Mojave desert tortoise) were classified as *Presumed Stable* to the effects of climate change by mid-21st century. *Presumed Stable* is defined as: "Available evidence does not suggest that abundance and/or range extent within the geographical area assessed will change (increase/decrease) substantially by 2050. Actual range boundaries may change." Mountain lion, Sonoran desert tortoise, and lowland leopard frog were not listed in the Nevada assessment. In addition, in a climate vulnerability assessment for the U.S. Department of Defense for species of concern on Arizona's Barry Goldwater Range, Bagne and Finch (2010) gave species a number score based on vulnerability or resilience to climate change across a number of functional traits. Of the three REA species on their list, Sonoran desert tortoise scored highest and most vulnerable with a score of 7 out of 10. Desert bighorn scored moderately vulnerable at 4.3, and Le Conte's thrasher more resilient at 2.4. For Mojave desert tortoise, Barrows (2011) modeled projected changes in tortoise distribution within Joshua Tree National Park and found the species to be sensitive and to have low capacity for adaptation to climate change, thus vulnerable in areas of high climate change exposure. With added vulnerability information such as these various results, one can analyze the vulnerability of particular species and communities with known sensitivities by overlaying the REA species' distributions with the climate change exposure map (Figure 5-39) and reassessing the exposure results with added vulnerability information. Bringing additional species sensitivity information to this analysis will allow the identification of locations where the species may experience various degrees of vulnerability to climate change as well as locations of possible refugia.

For the body of this report, results were posted in histograms as five climate change exposure classes for the 2045–2060 time period (Very High, High, Moderate, Moderately Low and Low). Results correspond to the percent of each species' or community's distribution potentially affected by climate change. An overlay map for each conservation element relative to climate change exposure can be found in Appendices B and C; the maps and source data may also be examined in greater detail on the data portal.

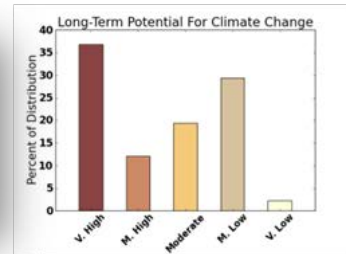
Each of the mammal and reptile species showed a unique signature to the climate model results (Figure 5-40). For the mammals, mountain lion showed the highest potential exposure to climate change with nearly 30% of its current distribution under the Very High category. Its major prey, mule deer and desert bighorn sheep, showed slightly less distribution area under the highest climate exposure category, but all three mammal species showed roughly 40% of their existing distributions under Very High or Moderately High exposure to climate change by 2045–2060. These mammals will be more likely to overcome some changes because of their wide-ranging nature and potential for dispersal, but increasing fragmentation or a reduction in the availability of their primary food or water sources may exacerbate the moderate direct effects of climate change on their habitat.

The Mojave desert tortoise (*G. agassizii*) exposure to climate change is very high with almost half of its current distribution under Very High or Moderately High exposure categories. The Sonoran desert tortoise (*G. morafkai*) has less exposure with roughly 30% of its current distribution within these same categories. Unlike the mammals, physiological impacts and dispersal limitations are more likely in the tortoise species. For example, temperature during egg maturation dictates the sex of the offspring (Spotila et al. 1994). With an increase in temperature, modifications in depth or aspect of burrows will be required if tortoises are to adapt to increasing ambient temperatures in the environment. (See more details on the desert tortoise species in the Desert Tortoise Case Study Insert.)

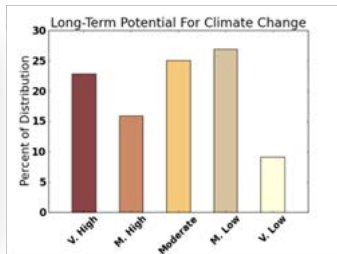
Mountain Lion



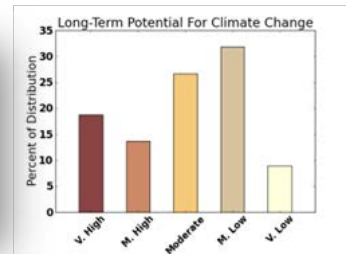
Desert Tortoise (*agassizii*)



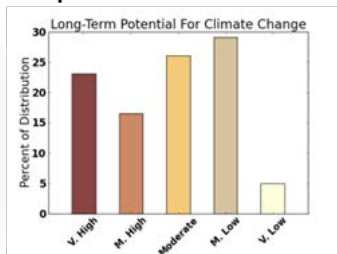
Mule Deer



Desert Tortoise (*morafkai*)



Desert Bighorn Sheep



Lowland Leopard Frog

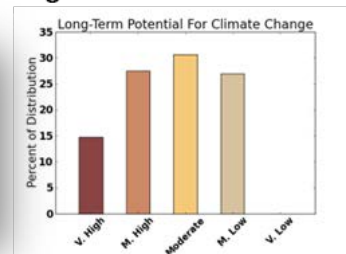
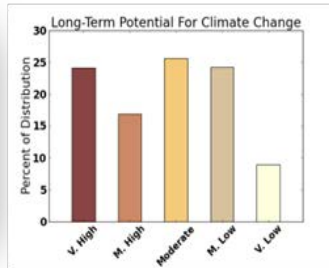


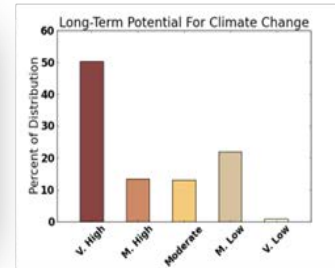
Figure 5-40. Potential exposure to climate change for mammals, reptiles, and the lowland leopard frog of the Sonoran Desert ecoregion.

Among bird species (Figure 5-41), 50% of the current distribution of the southwestern willow flycatcher is in the Very High climate change exposure category, followed by Le Conte’s thrasher (34%) and golden eagle (24%). Bell’s vireo showed the least exposure to climate change impacts, but it still had 30% of its current distribution in the Very High and Moderately High categories.

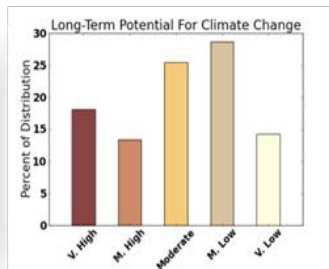
Golden Eagle



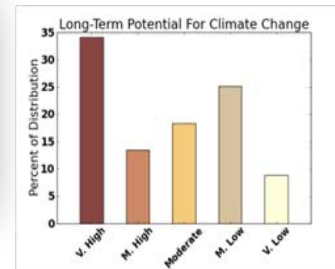
Southwest Willow Flycatcher



Lucy’s Warbler



LeConte’s Thrasher



Bell’s Vireo

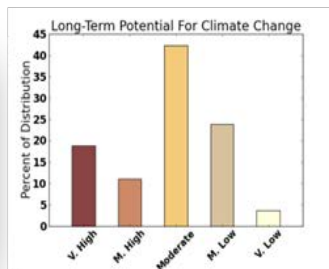
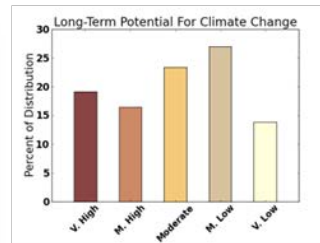


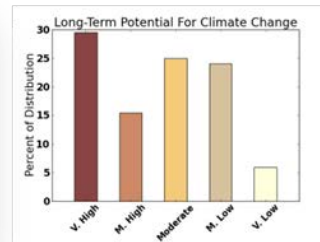
Figure 5-41. Potential exposure to climate change for birds of the Sonoran Desert ecoregion.

The vegetation community that showed the greatest percent area change under high climate change exposure was Sonoran-Mojave Creosotebush-White Bursage desert Scrub, followed by riparian vegetation and Sonoran Paloverde-Mixed Cacti Desert Scrub (Figure 5-42). With the vegetation communities, caution must be taken when interpreting these results as high exposure does not definitively mean decline; it means higher probability of change. Munson et al (2011), in a study using historical climate data in protected areas of the Sonoran Desert, project similar changes in vegetation communities; they found that with increasing mean annual temperatures there was a decline in velvet mesquite in mesic areas, a decline in foothills paloverde and ocotillo in more xeric foothills areas, and a decline in creosotebush in xeric shrublands.

Sonoran Paloverde-Mixed Cacti Desert Scrub



Sonora-Mojave Creosotebush-White Bursage Desert Scrub



Riparian Vegetation

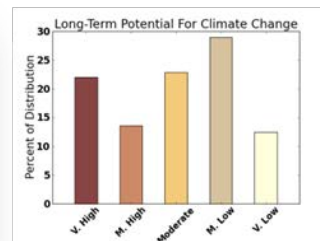


Figure 5-42. Potential exposure to climate change for the vegetation communities of the Sonoran Desert ecoregion.

Finally, existing designated sites showed fairly high vulnerability to climate change by 2060 with 42% of this category's land area under Very High or High exposure and nearly another 25% under Moderate exposure (Figure 5-43). Some of these sites may lose the function or features for which they were designated as a result of interactions among climate change and other change agents such as fire and invasive species. Future planning will be necessary to anticipate and mitigate possible changes to these valued designated sites.

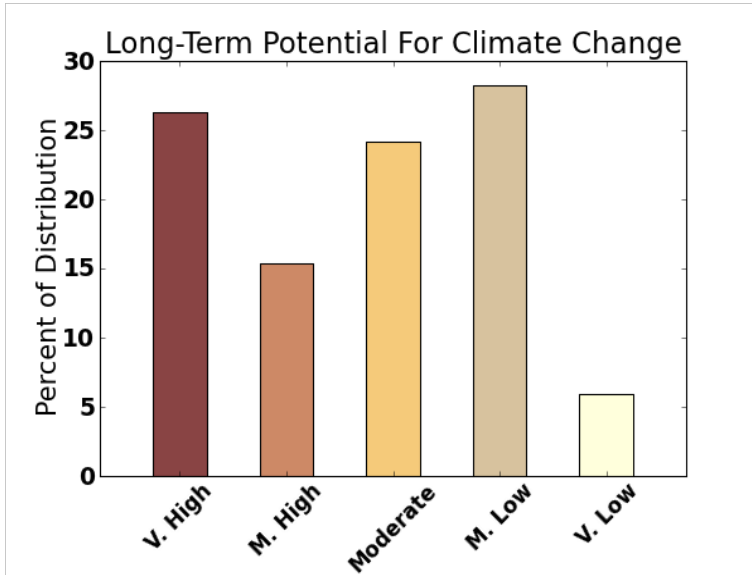


Figure 5-43. Potential exposure to climate change for the designated protected lands of the Sonoran Desert ecoregion.

5.4.2 References Cited

- Abatzoglou, J.T., and C.A. Kolden, 2011. Climate change in western U.S. deserts: Potential for increased wildfire and invasive annual grasses. *Rangeland Ecology and Management* 64(5): 471–478.
- Adger, W.N. 2006. Vulnerability. *Global Environmental Change* 16(3): 268–281.
- Archer, S.A., and K.I. Predick. 2008. Climate change and ecosystems of the Southwestern United States. *Rangelands* 30(3):23–38.
- Bagne, K.E., and D.M. Finch. 2010. An assessment of vulnerability of threatened, endangered, and at-risk species to climate change at the Barry M. Goldwater Range, Arizona. Department of Defense Legacy Program Report. 186 pp.
- Barrows, C.W. 2011. Sensitivity to climate change for two reptiles at the Mojave-Sonoran Desert interface. *Journal of Arid Environments* 75:629–635.
- Carter, T.R., R.N. Jones, X. Lu, S. Bhadwal, C. Conde, L.O. Mearns, B.C. O'Neill, M.D.A. Rounsevell, and M.B. Zurek. 2007. New assessment methods and the characterisation of future conditions. Pages 133–171 in Parry, M.L., O.F. Canziani, J.P. Palutikof, P.J. van der Linden, and C.E. Hanson (eds.), *Climate change 2007: Impacts, adaptation and vulnerability, Contribution of Working Group II to the Fourth Assessment Report of the Intergovernmental Panel on Climate Change*, Cambridge University Press, Cambridge, United Kingdom.

- Ehleringer, J.R. 2005. The influence of atmospheric CO₂, temperature, and water on the abundance of C₃/C₄ taxa. Pages 185–213 in Ehleringer, J.R., T.E. Cerling, and M.D. Dearing (eds.), *A history of atmospheric CO₂ and its effects on plants, animals, and ecosystems*. Springer, New York.
- Ehleringer, J.R., T.E. Cerling, and B.R. Helliker. 1997. C₄ photosynthesis, atmospheric CO₂, and climate. *Oecologia* 112:285–99.
- Füssel, H.M. 2007. Vulnerability: A generally applicable conceptual framework for climate change research. *Global Environmental Change* 17:155–167.
- Füssel, H.M., and R.J.T. Klein. 2006. Climate change vulnerability assessments: An evolution of conceptual thinking. *Climatic Change* 75 (3):301–329.
- Garfin, G., J. Eischeid, M. Lenart, K. Cole, K. Ironside, and N. Cobb. 2010. Downscaling climate projections to model ecological change on topographically diverse landscapes of the arid southwestern United States. Pages 21–44 in Van Riper, C., III, B.F. Wakeling, and T.D. Sisk (eds.), *The Colorado Plateau IV, Proceedings of the 9th Biennial Conference on Colorado Plateau Research, October, 2007*. University of Arizona Press.
- Glick, P., B.A. Stein, and N.A. Edelson. 2011. *Scanning the conservation horizon: A guide to climate change vulnerability assessment*. National Wildlife Federation, Washington D.C.
- Hostetler, S., J. Alder, and A. Allan. 2011. Dynamically downscaled climate simulations over North America: Methods, evaluation, and supporting documentation for users. Open-File Report 2011–1238, U.S. Geological Survey, Reston, Virginia.
- IPCC (Intergovernmental Panel on Climate Change). 2001. *Climate change 2001: Synthesis report. A Contribution of Working Groups I, II, and III to the Third Assessment Report of the Intergovernmental Panel on Climate Change*. Cambridge University Press, Cambridge, United Kingdom.
- Marshall, K.A. 1995. *Larrea tridentata* in Fire Effects Information System plants database, [Online]. U.S. Forest Service, Rocky Mountain Research Station, Fire Sciences Laboratory. <http://www.fs.fed.us/database/feis/>
- McAuliffe, J.R., and E.P. Hamerlynck. 2010. Perennial plant mortality in the Sonoran and Mojave deserts in response to severe, multi-year drought. *Journal of Arid Environments* 74:885–869.
- Morgan, J.A., D.R. LeCain, E. Pendall, D.M. Blumenthal, B.A. Kimball, Y. Carrillo, D.G. Williams, J. Heisler-White, F.A. Dijkstra, and M. West. 2011. C₄ grasses prosper as carbon dioxide eliminates desiccation in warmed semi-arid grassland. *Nature* 476: 202–206.
- Mote, P.W., D. Gavin, and A. Huyer. 2010. Climate change in Oregon’s land and marine environments. Chapter 1 in Dello, K.D., and P.W. Mote (eds.), *Oregon Climate Assessment Report*. College of Oceanic and Atmospheric Sciences, Oregon State University, Corvallis, Oregon.
- Munson, S., R. Webb, J. Belnap, and A. Hubbard. 2011. Forecasting climate change impacts to plant community composition in the Sonoran Desert region. *Global Change Biology* doi: 10.1111/j1365-2486.2011.02598.x.

- NNHP (Nevada Natural Heritage Program). 2011. Climate Change Vulnerability Index (Release 2.01). Nevada Natural Heritage Program, Carson City, Nevada.
- Ryan, M.G., and S.R. Archer. 2008. Land resources: Forests and arid lands: The effects of climate change on agriculture, land resources, water resources, and biodiversity in the United States. Final Report, Synthesis and Assessment Product 4.3. U.S. Climate Change Science Program and the Subcommittee on Global Change Research, Washington, D.C.
- Seager, R., M. Ting, I. Held, Y. Kushnir, J. Lu, G. Vecchi, H. Huang, N. Harnik, A. Leetmann, N. Lau, C. Li, J. Velez, and N. Naik. 2007. Model projections of an imminent transition to a more arid climate in southwestern North America. *Science* 316:1181–1184.
- Spotila, J.R., L.C. Zimmerman, C.A. Binckley, J.A. Grumbles, D.C. Rostal, A. List, Jr., E.C. Beyer, K.M. Phillips, and S.J. Kemp. 1994. Effects of incubation conditions on sex determination, hatching success, and growth of hatchling desert tortoises, *Gopherus agassizii*. *Herpetological Monographs* 8: 103–116.
- Theobald, D.M. 2010. Estimating natural landscape changes from 1992 to 2030 for the conterminous United States. *Landscape Ecology* 25(7):999–1011.
- Van Dyke, F.G., R.H. Brocke, H.G. Shaw, B.B. Ackerman, T.P. Hemker, and F.G. Lindzey. 1986. Reactions of mountain lions to logging and human activity. *The Journal of Wildlife Management* 50(1):95–102.
- Weis, J., and J. Overpeck. 2005. Is the Sonoran Desert losing its cool? *Global Change Biology* 11: 2065–2077, doi: 10.1111/j.1365-2486.2005.01020.x
- Young, B., E. Byers, K. Gravuer, K. Hall, G. Hammerson, and A. Redder. 2011. Guidelines for using the NatureServe Climate Change Vulnerability Index, Release 2.1. NatureServe, Arlington, VA.



Photo: Riparian fire on the lower Colorado River, BLM.